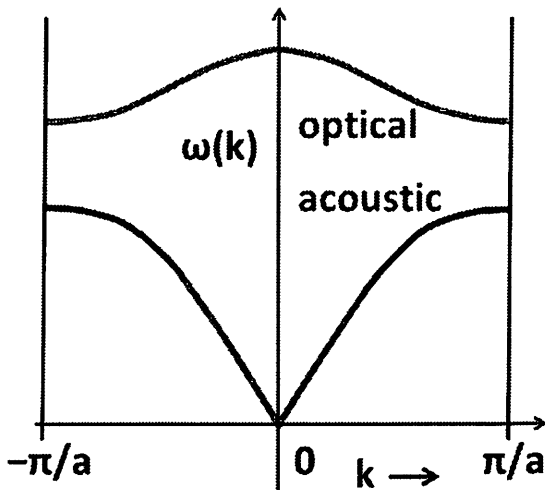


Problem 4.1)

a)

Goldstone theorem states that a broken continuous symmetry in presence of short range interactions results in collective mode of excitations that has no gap, which means the energy dispersion curve remains continuous even at 0 energy.

A typical classical example would be acoustic phonon because continuous rotational symmetry is broken during the formation of crystal.



Solutions to Assignment #4:

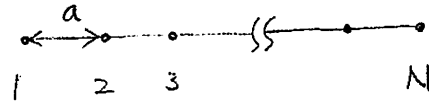
Three independent sets of solutions by:

- 1) Kevin Lee
- 2) Zach Zeigler
- 3) Sanjeev Kolli

Problem 4.1)

b)

$$S(\vec{q}) = \frac{1}{N} \left| \sum_j e^{i\vec{q} \cdot \vec{R}_j} \right|^2$$



where $\vec{q} = \vec{k}_{out} - \vec{k}_{in}$

\vec{q} is reciprocal lattice vector. Hence, it satisfies $\vec{q} \cdot \vec{R}_j = 2\pi n$.

$n = \text{integer}$.

Let's assume the lattice vector is a .

$$S(\vec{q}) = \frac{1}{N} \left| \sum_{n=1}^N e^{i\vec{q} n a} \right|^2$$

$$= \frac{1}{N} \left| e^{i\vec{q} a} + e^{2i\vec{q} a} + \dots + e^{N i\vec{q} a} \right|^2$$

$$= \frac{1}{N} |e^{i\vec{q} a}|^2 \left| 1 + e^{i\vec{q} a} + \dots + e^{(N-1)i\vec{q} a} \right|^2$$

$$= \frac{1}{N} \left| \frac{(1 - e^{N i\vec{q} a})}{1 - e^{i\vec{q} a}} \right|^2$$

$$= \frac{1}{N} \left(\frac{1 - e^{N i\vec{q} a}}{1 - e^{i\vec{q} a}} \right) \left(\frac{1 - e^{-N i\vec{q} a}}{1 - e^{-i\vec{q} a}} \right)$$

$$= \left(\frac{1}{N} \right) \left(\frac{1 - e^{N i\vec{q} a} - e^{N i\vec{q} a} + 1}{1 - e^{-i\vec{q} a} - e^{i\vec{q} a} + 1} \right) = \left(\frac{1}{N} \right) \left(\frac{2 - 2\cos(N\vec{q} a)}{2 - 2\cos(\vec{q} a)} \right)$$

Note: $2 \sin^2 \alpha = 1 - \cos 2\alpha$

$$= \left(\frac{1}{N} \right) \frac{\sin^2 \left(\frac{N\vec{q} a}{2} \right)}{\sin^2 \left(\frac{\vec{q} a}{2} \right)}$$

#

Problem 4.1)

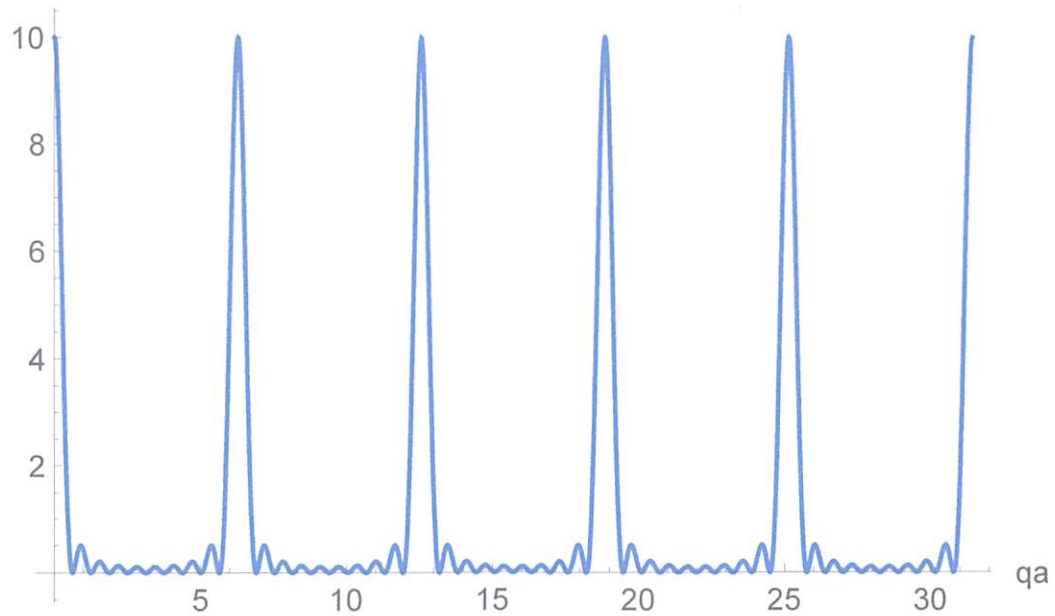
c) According to the structure factor equation for 1D perfect lattice.

$$S(q) = \frac{1}{N} \frac{\sin^2(\frac{Naq}{2})}{\sin^2(\frac{aq}{2})}$$

We can plot the structure factor by Mathematica.

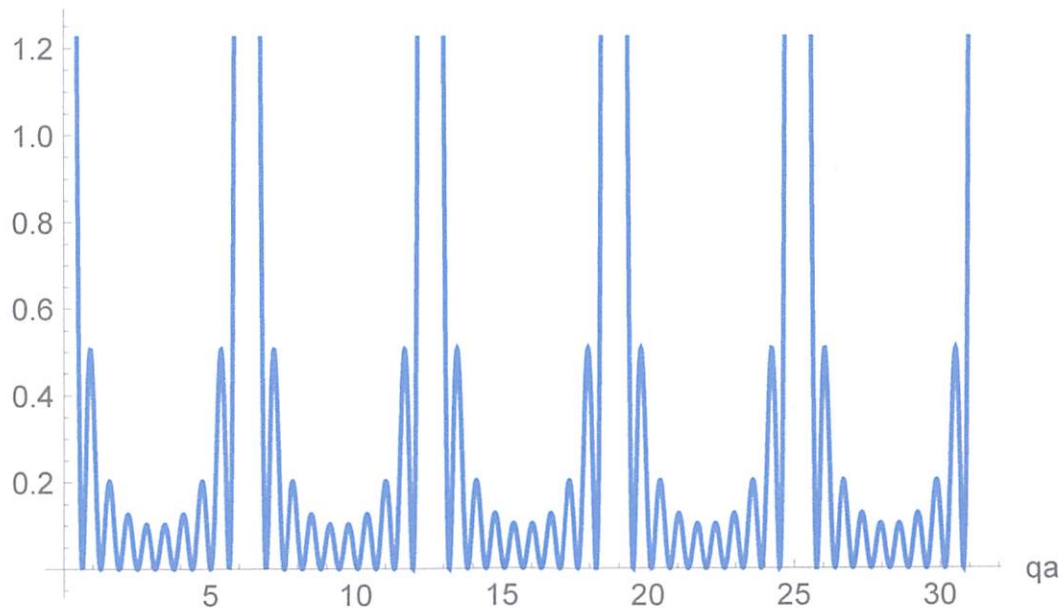
This is the plot of N=10 atoms.

Structural factor



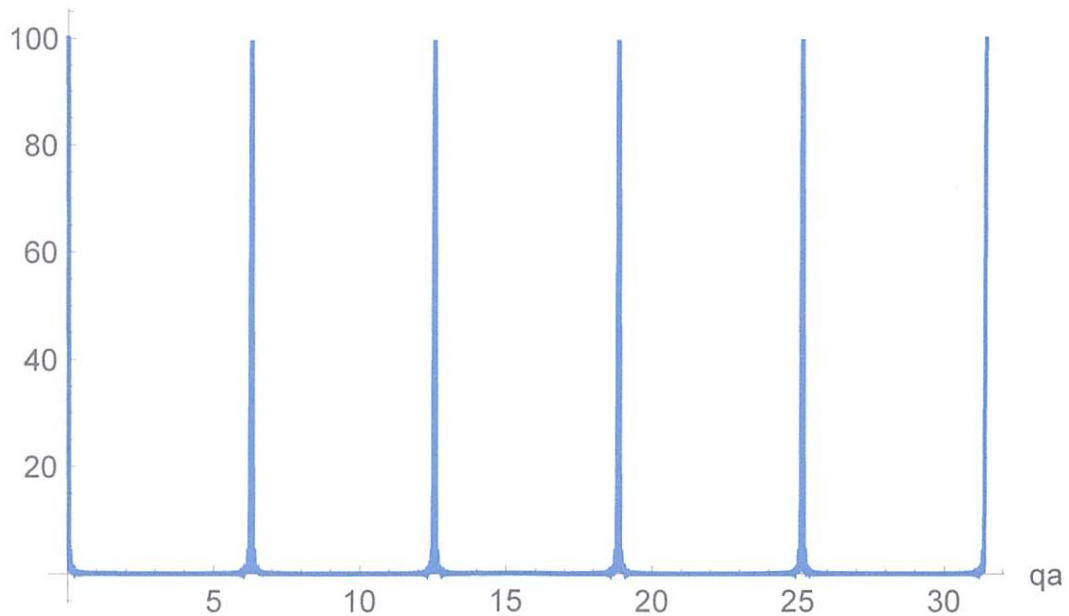
If we zoom in, the following figure, we can see there are 10 peaks in between maximum peaks. And the maximum peak value is 10.

Structural factor



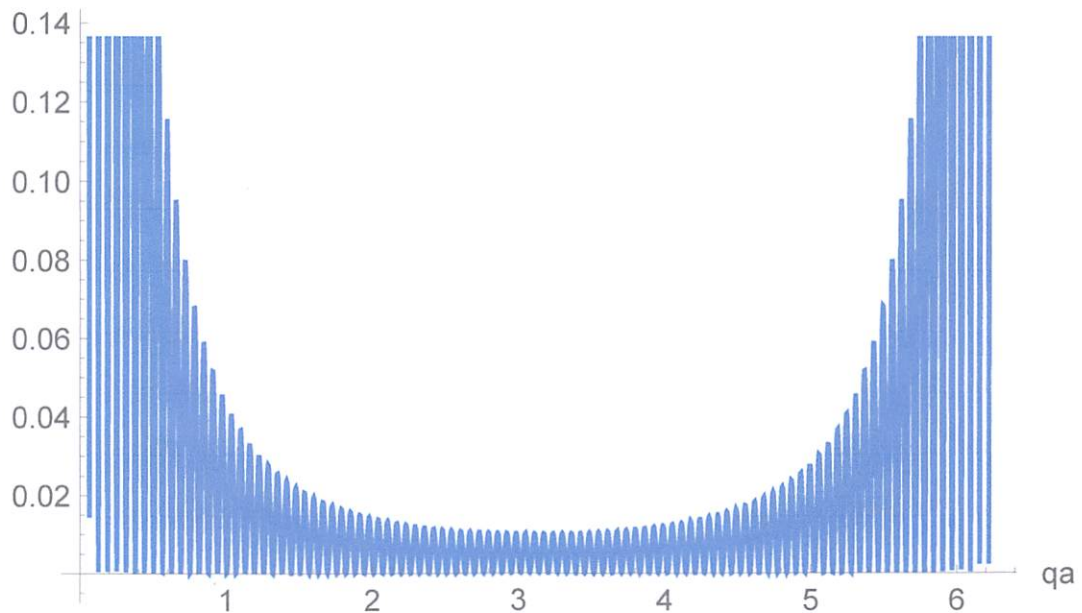
Then I made the plot of $N=100$.

Structural factor



If we zoom in for $0 < qa < 2\pi$, we can see the small satellite peaks in between.

Structural factor



- To prove the structure factor's maximum value, we need to observe the behavior of the sine function.

First, when $\frac{qa}{2} = n\pi$, " n " is an integer, the function $\sin(\frac{aq}{2})$ goes to zero. But

the structure is not divergent since $\sin(\frac{Naq}{2})$ also has zero value.

To get the value of $\frac{\sin(\frac{Naq}{2})}{\sin(\frac{aq}{2})}$, we need L' Hospital's rule.

L' Hospital's Rule

Suppose $f(c) = g(c) = 0$, and $g'(x) \neq 0$.

$$\lim_{x \rightarrow c} \frac{f(x)}{g(x)} = \lim_{x \rightarrow c} \frac{f'(x)}{g'(x)}$$

Therefore, we have

$$\lim_{\frac{aq}{2} \rightarrow 0} \frac{\sin(\frac{Naq}{2})}{\sin(\frac{aq}{2})} = \lim_{\frac{aq}{2} \rightarrow 0} \frac{N \cos(\frac{Naq}{2})}{\cos(\frac{aq}{2})} = N$$

$$S(q = 0) = \frac{1}{N} \times N^2 = N$$

Hence, we proved that the maximum value is “N” for structure factor.

- Now we prove that there are N peaks in between two maximum peaks.

Effectively, each peak lies in between two consecutive minimum.

Therefore, we can calculate peak number based on the number of minimum points in between 0 and 2π .

When the function has zero values, it means $\sin^2\left(\frac{Nqa}{2}\right) = 0$.

$$\frac{N}{2} \times qa = n\pi, \text{ where } n = \text{integers}$$

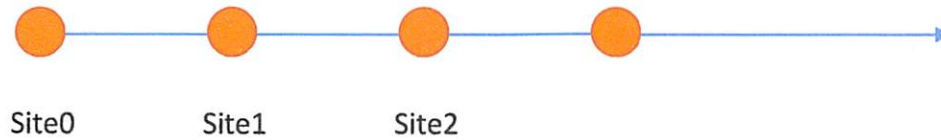
$$qa = \frac{2\pi n}{N}$$

It is obvious that $n = 0, 1, 2, 3, \dots, N$, then $qa = 0 \rightarrow 2\pi$. So the total satellite peaks including the two maximum peaks is exactly “N”.

Or we can argue this problem in another way, looking how many maximum values for qa in between 0 and 2π . Basically, it's the same problem.

Problem 4.1)

d) Now we need to remove three atoms randomly in the 1D lattice. The 1D lattice can be viewed as following.



I chose to remove the site 2,5 and 8 atoms. If we look at the original structure factor equation instead of the calculated form in problem 4.1c. The form is easier to understand. This is the original structure factor without vacancies.

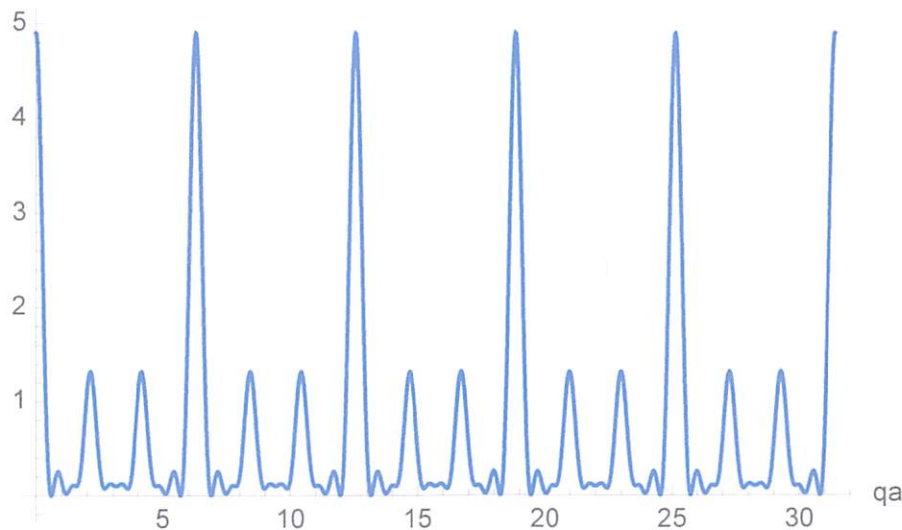
$$S(q) = \frac{1}{N} \left| \sum_{n=0}^{N-1} e^{iqna} \right|^2$$

If we want to add vacancies, we can just plug in the minus lattice site term in the above expression.

$$S(q) = \frac{1}{N} \left| -e^{2iqa} - e^{5iqa} - e^{8iqa} + \sum_{n=0}^{N-1} e^{iqna} \right|^2$$

So we can make the plot for N=10.

Structure factor

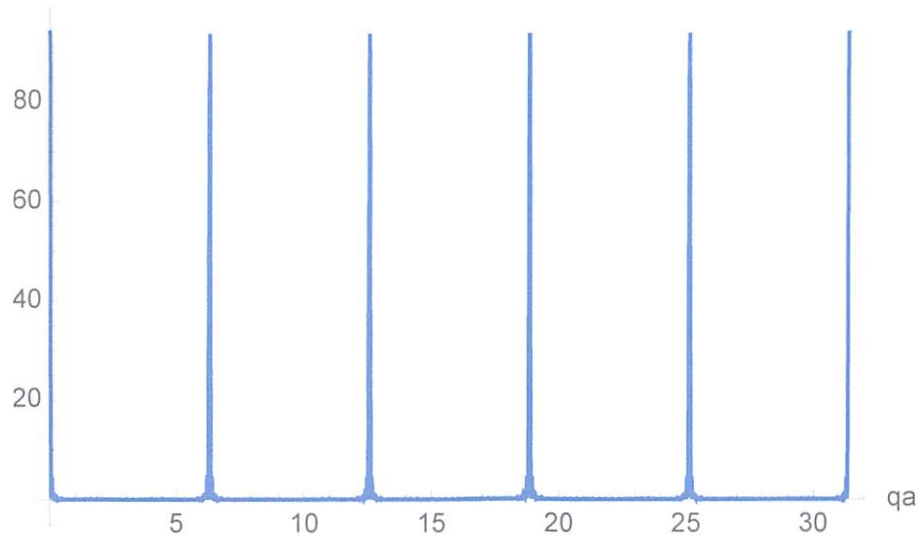


This maximum peaks' intensities are decreased. If we calculated the peaks in between the two maximum peaks, there are still 10 peaks.

For $N=100$, I chose site 2, 50, 77 to be vacancies.

$$S(q) = \frac{1}{N} \left| -e^{2iqa} - e^{50iqa} - e^{77iqa} + \sum_{n=0}^{N-1} e^{inqa} \right|^2$$

Structure factor



I would say that diffraction experiment is a good tool to determine the crystal quality of a semiconductor. From these calculations, we can see that as long as there are vacancies in the crystal, the diffraction peaks' intensity decreased. But I wouldn't say it's good for determining exact number of vacancies in the crystal. It is only suitable to compare two identical crystals' quality. The one with higher diffraction peaks has better crystal quality, which means less vacancies here.

Problem 4.2)

$$a) \quad \vec{R}_j \rightarrow \vec{R}_j + \vec{u}_j(t) \quad \vec{R}_k \rightarrow \vec{R}_k + \vec{u}_k(t)$$

$$\begin{aligned} S(\vec{q}, T) &= \frac{1}{N} \left| \sum_j e^{i\vec{q} \cdot (\vec{R}_j + \vec{u}_j(t))} \right|^2 \\ &= \frac{1}{N} \sum_j e^{i\vec{q} \cdot (\vec{R}_j + \vec{u}_j)} \cdot \sum_k e^{i\vec{q} \cdot (\vec{R}_k + \vec{u}_k)} \quad \text{For simplicity, I drop the time here.} \\ &= \frac{1}{N} \sum_j \sum_k e^{i\vec{q} \cdot (\vec{R}_j - \vec{R}_k)} \cdot e^{i\vec{q} \cdot (\vec{u}_j - \vec{u}_k)} \\ &= \left(\frac{1}{N} \right) \left[\sum_{j=k}^N e^{i\vec{q} \cdot 0} \cdot e^{i\vec{q} \cdot 0} + \sum_{j \neq k}^N e^{i\vec{q} \cdot (\vec{R}_j - \vec{R}_k)} \cdot e^{i\vec{q} \cdot (\vec{u}_j - \vec{u}_k)} \right] \\ &= 1 + \frac{1}{N} \sum_{j \neq k}^N e^{i\vec{q} \cdot (\vec{R}_j - \vec{R}_k)} \cdot e^{i\vec{q} \cdot (\vec{u}_j - \vec{u}_k)} \\ &= \left(\frac{1 + \frac{1}{N} \sum_{j \neq k}^N e^{i\vec{q} \cdot (\vec{R}_j - \vec{R}_k)} \cdot e^{i\vec{q} \cdot (\vec{u}_j - \vec{u}_k)}}{e^{i\vec{q} \cdot \sum_{j,k} (\vec{u}_j - \vec{u}_k)}} \right) e^{i\vec{q} \cdot \sum_{j,k} (\vec{u}_j - \vec{u}_k)} \end{aligned}$$

Note: $\sum_{j,k} (\vec{u}_j - \vec{u}_k) = \sum_{j \neq k} (\vec{u}_j - \vec{u}_k) \quad \therefore \sum_{j=k} (\vec{u}_j - \vec{u}_k) = 0$

$$= e^{i\vec{q} \cdot \sum_{j,k} (\vec{u}_j - \vec{u}_k)} \left[e^{-i\vec{q} \cdot \sum_{j \neq k} (\vec{u}_j - \vec{u}_k)} + \frac{1}{N} \sum_{j \neq k}^N e^{i\vec{q} \cdot (\vec{R}_j - \vec{R}_k)} \cdot e^{i\vec{q} \cdot (\vec{u}_j - \vec{u}_k)} \cdot e^{-i\vec{q} \cdot \sum_{j \neq k} (\vec{u}_j - \vec{u}_k)} \right]$$

Since j, k are independent each other, $\vec{q} \cdot (\vec{u}_j - \vec{u}_k) = 0$ for time average.

$$= e^{i\vec{q} \cdot \sum_{j,k} (\vec{u}_j - \vec{u}_k)} \left[1 + \frac{1}{N} \sum_{j \neq k}^N e^{i\vec{q} \cdot (\vec{R}_j - \vec{R}_k)} \right]$$

$$= S(\vec{q}, T=0) e^{i\vec{q} \cdot \sum_{j,k} (\vec{u}_j - \vec{u}_k)}$$

Problem 4.d)

b) From a), we have $\vec{S}(\vec{q}, T) = \vec{S}(\vec{q}, T=0) e^{i \vec{q} \cdot \sum_{j,k} (\vec{u}_j(t) - \vec{u}_k(t))}$

$$(*) e^{i \vec{q} \cdot \sum_{j,k} (\vec{u}_j - \vec{u}_k)} = 1 + i \vec{q} \cdot \sum (\vec{u}_j - \vec{u}_k) - \frac{1}{2} \left(\vec{q} \cdot \sum (\vec{u}_j - \vec{u}_k) \right)^2 + \dots$$

Assume each lattice point oscillate independently.

$$\Rightarrow \vec{q} \cdot \sum (\vec{u}_j - \vec{u}_k) = 0$$

Assume the angle between \vec{q} and $\vec{u}_j - \vec{u}_k$ is " θ ".

$$\frac{1}{2} \left(\vec{q} \cdot \sum (\vec{u}_j - \vec{u}_k) \right)^2 = \frac{1}{2} \langle \cos^2 \theta \rangle q^2 \sum |\vec{u}_j - \vec{u}_k|^2$$

$$= \frac{1}{2} \langle \cos^2 \theta \rangle q^2 \sum (|\vec{u}_j|^2 + |\vec{u}_k|^2 - 2 \vec{u}_j \cdot \vec{u}_k)$$

$\sum_{j,k} \vec{u}_j(t) \cdot \vec{u}_k(t) = 0$ because different lattice points are independently oscillating.

$$= \frac{1}{2} \langle \cos^2 \theta \rangle q^2 \sum_j 2 |\vec{u}_j|^2$$

$\frac{1}{3}$ geometrical average over a sphere.

$$= \frac{1}{2} \cdot \frac{1}{3} \cdot 2 \sum_j |\vec{u}_j|^2 q^2 = \frac{1}{3} \sum_j |\vec{u}_j|^2 q^2$$

$$(*) \approx 1 - \frac{1}{3} q^2 \sum_j |\vec{u}_j|^2 + \dots$$

$$\approx e^{-\frac{1}{3} q^2 \sum_j |\vec{u}_j|^2}$$

Problem 4.2)

b) Now we need to solve $\sum_j |\vec{u}_j|^2$.

For a simple harmonic oscillator, energy is the following.

$$\frac{1}{2} M \omega_0^2 \sum_j |\vec{u}_j|^2 = \frac{3}{2} k_B T$$

↑
3D thermal average energy

$$\sum |\vec{u}_j|^2 = \frac{3 k_B T}{M \omega_0^2}$$

$$(*) = e^{-\frac{1}{2} q^2 \cdot \frac{3 k_B T}{M \omega_0^2}} = e^{-\frac{q^2 k_B T}{M \omega_0^2}}$$

$$\Rightarrow S(\vec{q}, T) \approx S(\vec{q}, T=0) e^{-\frac{q^2 k_B T}{M \omega_0^2}}$$

c) For 1D case, we need to modify two things in the previous derivation.

1. Thermal average energy = $\frac{1}{2} k_B T$

2. Geometrical average $\langle \cos^2 \theta \rangle = 1$

$$\Rightarrow (*) = 1 - \frac{1}{2} \cdot 1 \cdot q^2 \cdot 2 \sum_j |\vec{u}_j|^2 + \dots$$

$$\left(\sum_j |\vec{u}_j|^2 = \frac{k_B T}{M \omega_0^2} \right)$$

$$= 1 - \frac{q^2 k_B T}{M \omega_0^2} + \dots$$

$$\approx e^{-\frac{q^2 k_B T}{M \omega_0^2}}$$

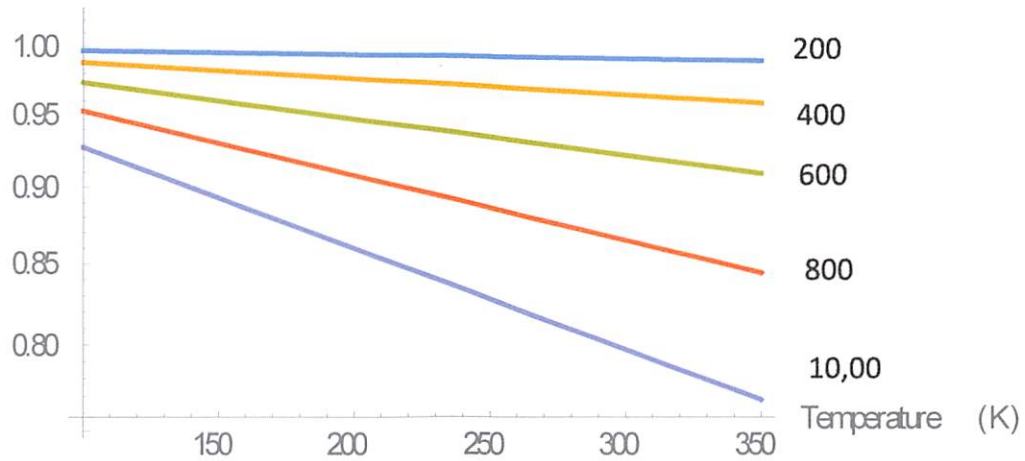
$$\Rightarrow S(\vec{q}, T) = S(\vec{q}, T=0) e^{-\frac{q^2 k_B T}{M \omega_0^2}}$$

Problem 4.2)

d)

First, we can plot the similar figure with the 1D lattice structure.

Normalized Structure factor



Although the 1D lattice model is not correct for Al, we can capture the main characteristics of the measurement data.

The \mathbf{q} vector is the reciprocal lattice vector. In 3D system, it can be written as following form.

$$\mathbf{q} = h\mathbf{b}_1 + k\mathbf{b}_2 + l\mathbf{b}_3$$

h, k, l are the Miller index. $\mathbf{b}_1, \mathbf{b}_2$ and \mathbf{b}_3 are the reciprocal lattice vectors.

$$\mathbf{b}_1 = \frac{2\pi}{a}$$

When we change the injection angle of X-Ray, we are observing different planes of the crystal. When the crystal plane's Miller index is larger, the Debye Waller factor will decrease.

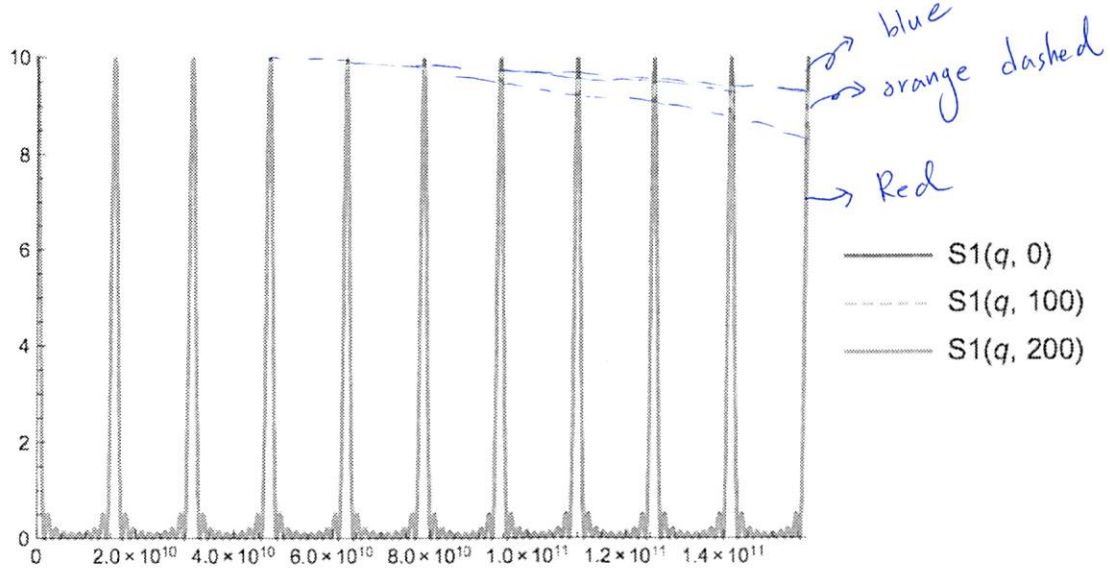
$$\mathcal{S}(\mathbf{q}, T) = \mathcal{S}(\mathbf{q}, T = 0) e^{\frac{-k_B T q^2}{M \omega_0^2}}$$

$$h \uparrow, q \uparrow, e^{\frac{-k_B T q^2}{M \omega_0^2}} \downarrow, \mathcal{S}(\mathbf{q}, T) \downarrow$$

This characteristic is shown in the figure. (10, 0, 0) has the smallest value.

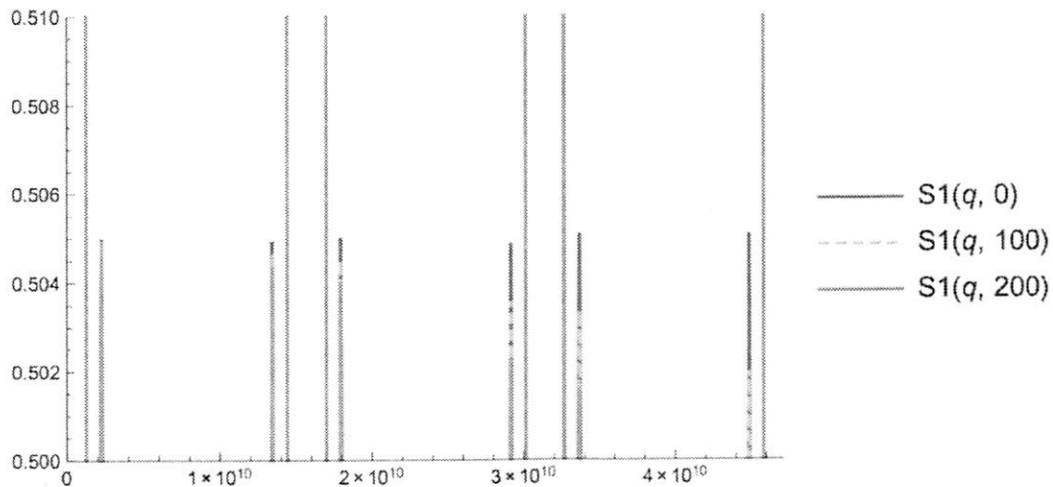
As the temperature increases, the exponential factor will decrease further, too. The structure factor will decrease accordingly.

The figure above is calculated by the first maximum peak's intensity. If we make plots of structure factor for different temperature, we can see the peak intensity decreasing as q value increases, which is the same thing for increasing Miller index discussed here.



The blue line is structure factor for zero K. Orange dashed line is structure factor for 100K. Red line is structure factor for 200K. The horizontal axis is the q vector.

As we increase Miller index, q vector value increases, which means moving along positive x direction in the plot. We can there is a drop in the peak intensity as q increasing. In addition, the peak intensity decreases as the temperature rises. Both observations are consistent with the provided plot in the problem.



This is a zoom in image of the above diagram. The satellite peaks are also decreasing.

Problem 4.2)

e)

If we want to utilize the temperature dependence of structure factor, the best scenario is that the intensity variation is large when temperature changes.

From Debye Waller factor, we can analyze the problem.

$$S(\mathbf{q}, T) \propto e^{\frac{-k_B T q^2}{M \omega_0^2}}$$

In order to have large variations, we can choose materials with smaller mass or smaller resonant frequency.

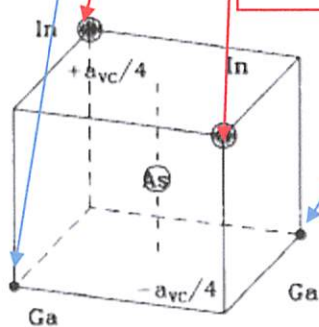
The other strategy would be using large Miller's index peaks as reference. This is similar to our argument in the previous problem. Large Miller's index corresponds to larger q value, and this makes exponential term more sensitive to temperature.

Problem 4.3)

a)

If we want to generate the fig. 3, we need to first determine the strain energy dependence on the composition as the fig 2.

To generate this plot, we need to consider the microscopic strain and bending energies of different configuration. The total microscopic energy can be written according to Chapter 4 of Taso's book. For Type 2 configuration, we can write down as following.

$$\begin{aligned}
 u \approx & \frac{3}{4} \alpha_{GaAs} \left[\frac{\sqrt{3}}{4} a_{VC} - d_{GaAs,0} + \frac{z}{\sqrt{3}} \right]^2 + \frac{3}{4} \alpha_{GaAs} \left[\frac{\sqrt{3}}{4} a_{VC} - d_{GaAs,0} + \frac{z}{\sqrt{3}} \right]^2 \\
 & + \frac{3}{4} \alpha_{InAs} \left[\frac{\sqrt{3}}{4} a_{VC} - d_{InAs,0} - \frac{z}{\sqrt{3}} \right]^2 \\
 & + \frac{3}{4} \alpha_{InAs} \left[\frac{\sqrt{3}}{4} a_{VC} - d_{InAs,0} - \frac{z}{\sqrt{3}} \right]^2 \\
 & + \frac{3}{16} \beta_{GaAs} \left[\frac{-2}{3} \left(\frac{\sqrt{3}}{4} a_{VC} - d_{GaAs,0} + \frac{2z}{\sqrt{3}} \right) \right]^2 \\
 & + \frac{3}{16} \beta_{GaAs} \left[\frac{-2}{3} \left(\frac{\sqrt{3}}{4} a_{VC} - d_{GaAs,0} + \frac{2z}{\sqrt{3}} \right) \right]^2 \\
 & + \frac{3}{16} \beta_{InAs} \left[\frac{-2}{3} \left(\frac{\sqrt{3}}{4} a_{VC} - d_{InAs,0} - \frac{2z}{\sqrt{3}} \right) \right]^2 \\
 & + \frac{3}{16} \beta_{InAs} \left[\frac{-2}{3} \left(\frac{\sqrt{3}}{4} a_{VC} - d_{InAs,0} - \frac{2z}{\sqrt{3}} \right) \right]^2
 \end{aligned}$$


If we want to calculate different configuration, we just change the alpha, beta constants, and the equilibrium bond length. Red box terms correspond "In" atom position. Blue box terms correspond to "Ga" atom position.

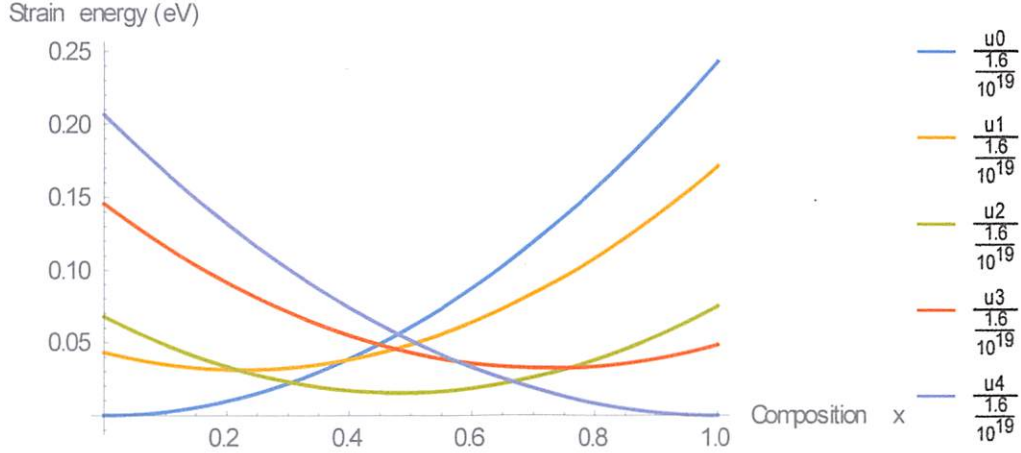
To find each configuration's equilibrium energies, we can take derivative of z to the strain energy.

$$\frac{\partial u}{\partial z} = 0$$

We will find an equilibrium value of z , then substitute this value into total strain energy equation. We have the strain energy of each configuration.

Note that $a_{VC} = (1 - x)a_{InAs} + xa_{GaAs}$, which is the virtual crystal approximation.

Now we can make strain energy plot.



" u_i " is the total strain energy of configuration " i ". From this diagram, we can see that the strain energy is composition dependent.

For completely random atom distribution, the plot is very easy.

$$\alpha_i x^{4-i} (1-x)^i$$

This is the proportion of " i " configuration.

To get the Fig 3. in the paper, we need to consider the strain energy into free energy and use Lagrange multiplier to get the equilibrium distribution of each configuration. Basically, we have to solve Eq. 12 in the paper.

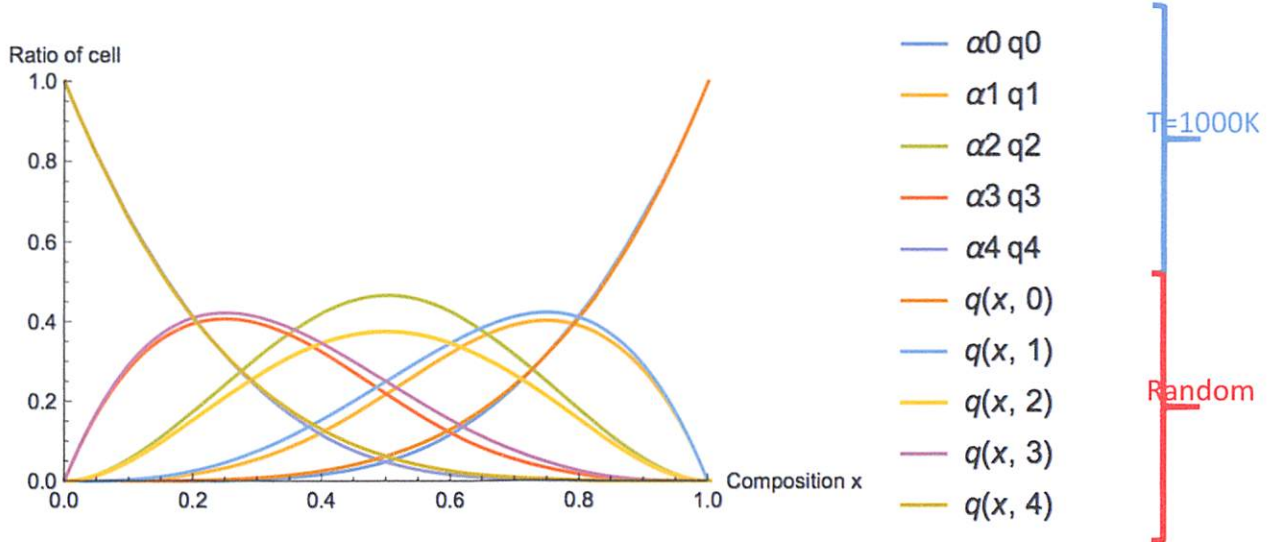
$$(1-x)\eta_0 t^4 + (3-4x)\eta_1 t^3 + (3-6x)\eta_2 t^2 + (1-4x)\eta_3 t^1 - x\eta_4 = 0$$

where $\eta_i = e^{\frac{-\epsilon_i}{k_B T}}$ and $t = e^{\frac{-b}{4k_B T}}$. " ϵ_i " is the strain energy of i th configuration. " b " is

a constant to be solved in the equation. For simplicity, I solved " t " in the equation instead of " b " since it's too complicated to solve " b " directly. Since it is a forth order equation, there will be four solutions. But there is only one solution can give us the final result. After solving " t ", we can get the ratio of each configurations as following.

$$\alpha_i q_i = \alpha_i c \eta_i t^{4-i}$$

" c " is a normalization constant calculated by $c^{-1} = \sum \eta_i t^{4-i} \alpha_i$. If we solve all the parameters above, we can draw the diagrams in the paper.

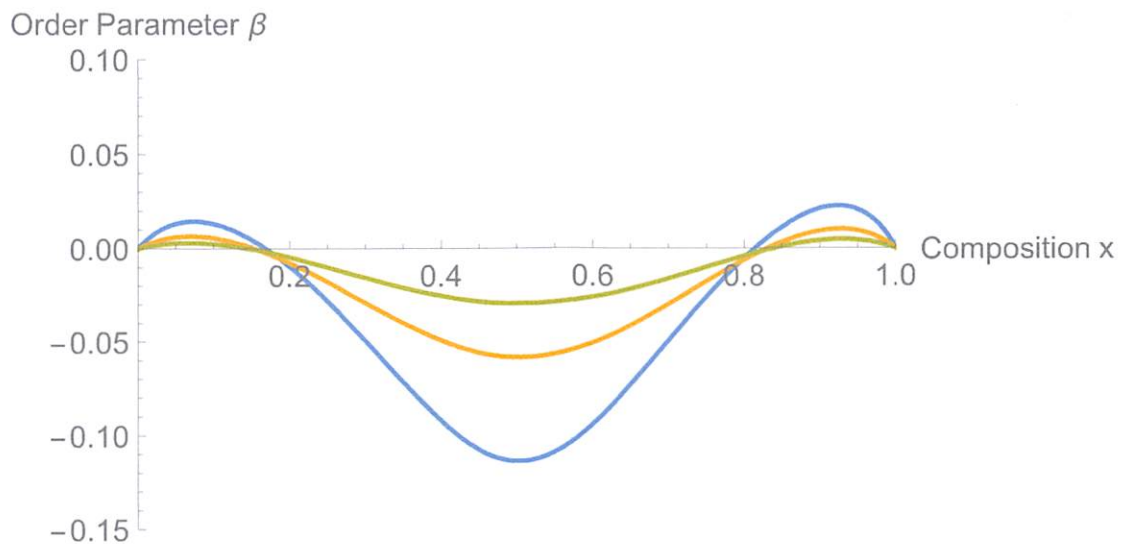


Each sub-index in the plot means the i th configuration. So the figure tells us that for type 1,2,3 when temperature increases, the ratio of each configuration increases. While for type 0 and 4, the trend is opposite.

For the order parameter, I used the equation 14 in the paper.

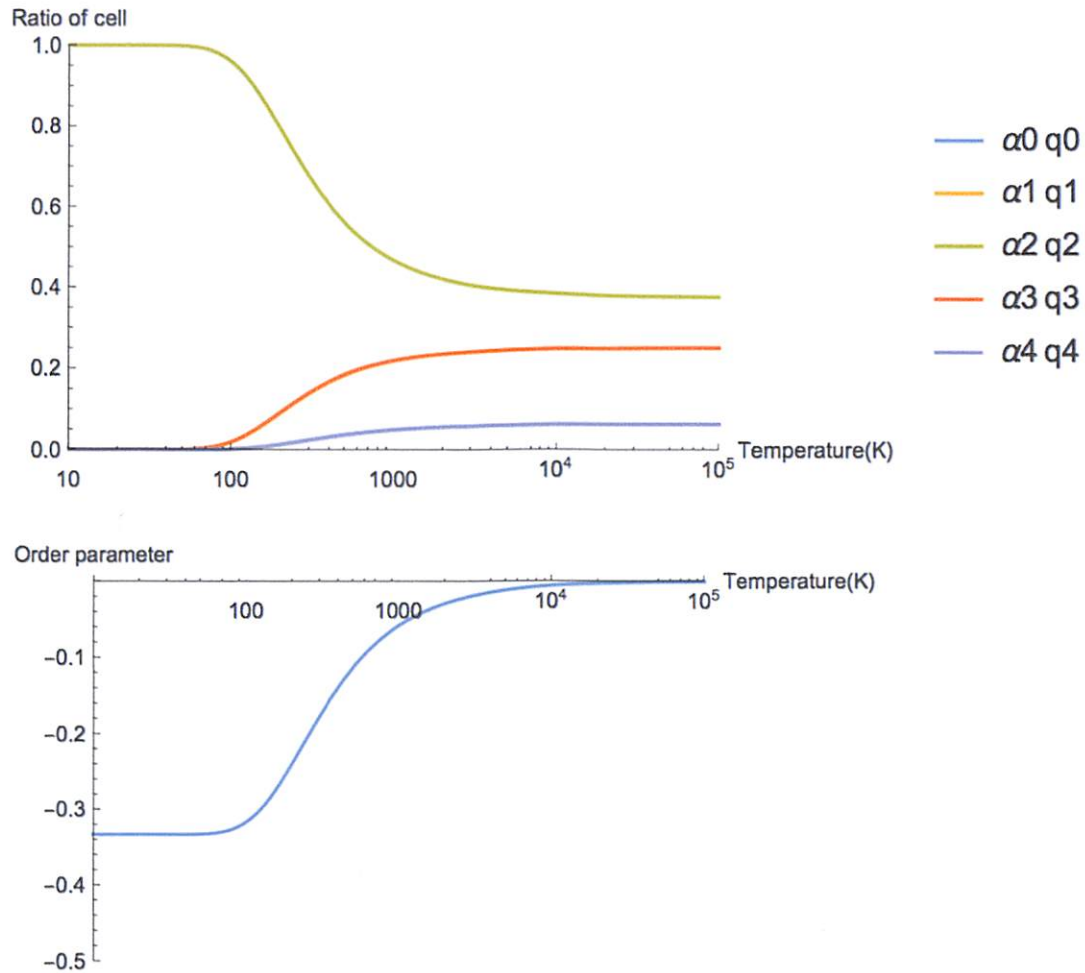
$$\beta = 1 - \frac{q_1 + 2q_2 + q_3}{x(1-x)}$$

However, the results of my calculation seems a little bit different from the paper's results.



Blue line corresponds to $T=500K$. Orange corresponds to $T=1000K$. Green corresponds to $T=2000K$. At very low x and very high x , order parameters seem to have positive values, indicating the alloy tends to form cluster at these compositions. I will discuss why there is a discrepancy here later.

For Fig 5, I split it into two figures for convenience. These are the results for composition $x=0.5$, which means for $In_{0.5}Ga_{0.5}As$. The only difference for these two plots is that it is assumed for fixed composition x .



We can see from the top diagram. When temperature increases, type 2 configuration starts decreasing, while type 1,3 and 0,4 are both increasing. As the temperature reaches very high value, the alloy tends to form cluster instead of having short-range ordering.

Now I discussed about why there is a little discrepancy in the order parameter plot. The primary reason comes from the strain energy. When I am using the equation in Taso's chapter, the total strain energy has already been simplified. The total energy's dependence on position of As in the tetrahedron, which is z , has only considered up to the second order. That's why the strain energy dependence on composition x is not completely resembles paper's results. And this later make an influence on the order parameter plot.

Problem 4.3)

b)

The primary point in this paper is that III-V ternary alloys tend to have short range order instead of clustering. Traditionally, when we are discussing the III-V alloy, we used the virtual crystal approximation or assumed the atom positions are completely random. But experimentally, there are reports saying that there is short-range order.

The enthalpy of traditional strain energies is based on virtual crystal approximation, which is four times larger than the experimental values. To get a more accurate results, we can use different tetrahedron configurations to calculate the strain energies and then plug into the enthalpy. And we have to take both bond-length deviation and bond angle distortion into strain energy calculations.

Entropy is the primary difference for this configuration method. The strain energy is stored in the bonds between the nearest atom's bond. Writing down the free energy and Lagrange multiplier can give us the equilibrium configuration ratio. From Fig3, we can see that there is an ordering occurs when temperature increases. Take $x=0.5$ for instance. We can see type2 ratio is slightly increased, while type 0 and 4 decreases.

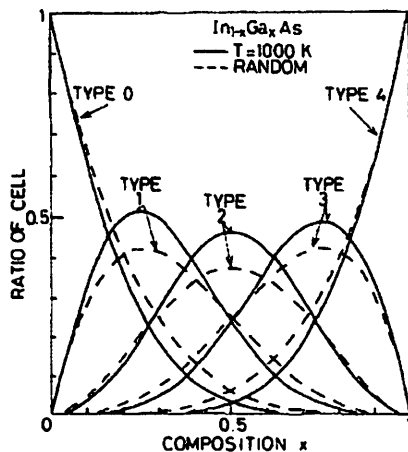


FIG. 3. Fractional values of five tetrahedron cells. Broken line: random arrangement. Solid line: at $T = 1000$ K for $\text{In}_{1-x}\text{Ga}_x\text{As}$.

From the order parameter plot, we can see that as we increase the temperature, the parameter goes to negative value, which means there is ordering when temperature is increasing.

Alloy tends to order at low temperature since the entropy contribution is very small in the free energy. Enthalpy dominates and tends to have more order to minimize the energy. As temperature increases, the order becomes little. Basically,

for all the alloys between two composite binary compounds, the order parameter is negative, which means they tend to have short range order.

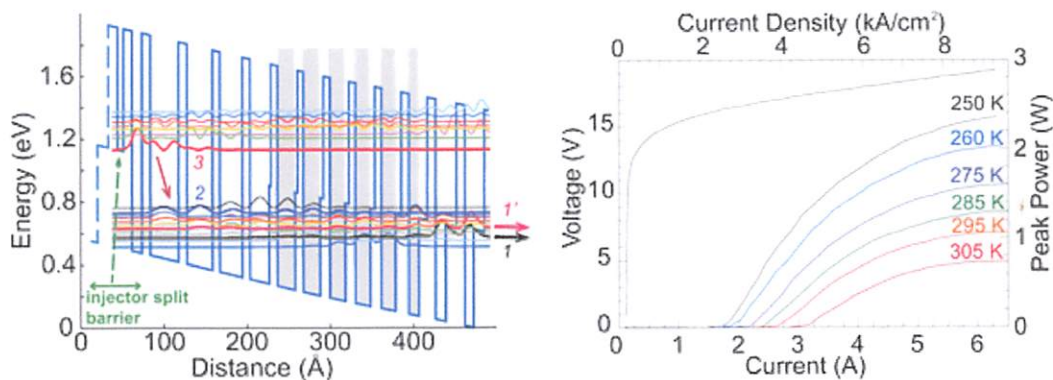
From all these results, they concluded if there compositional fluctuation in the alloy, it will be suppressed in equilibrium state since fluctuation has larger strain energy. And the short range ordering is preferred instead of clustering.

c)

Since tuning these alloy's composition can result in bandgap offset, a lot of research utilized these features to create optical devices. Using these alloys, researcher can create quantum wells in the growing process. Like the discussion in the class before, quantum well structure can enhance the carrier recombination (joint density of states). Either interband or intersubband optical devices had been developed based on these materials.

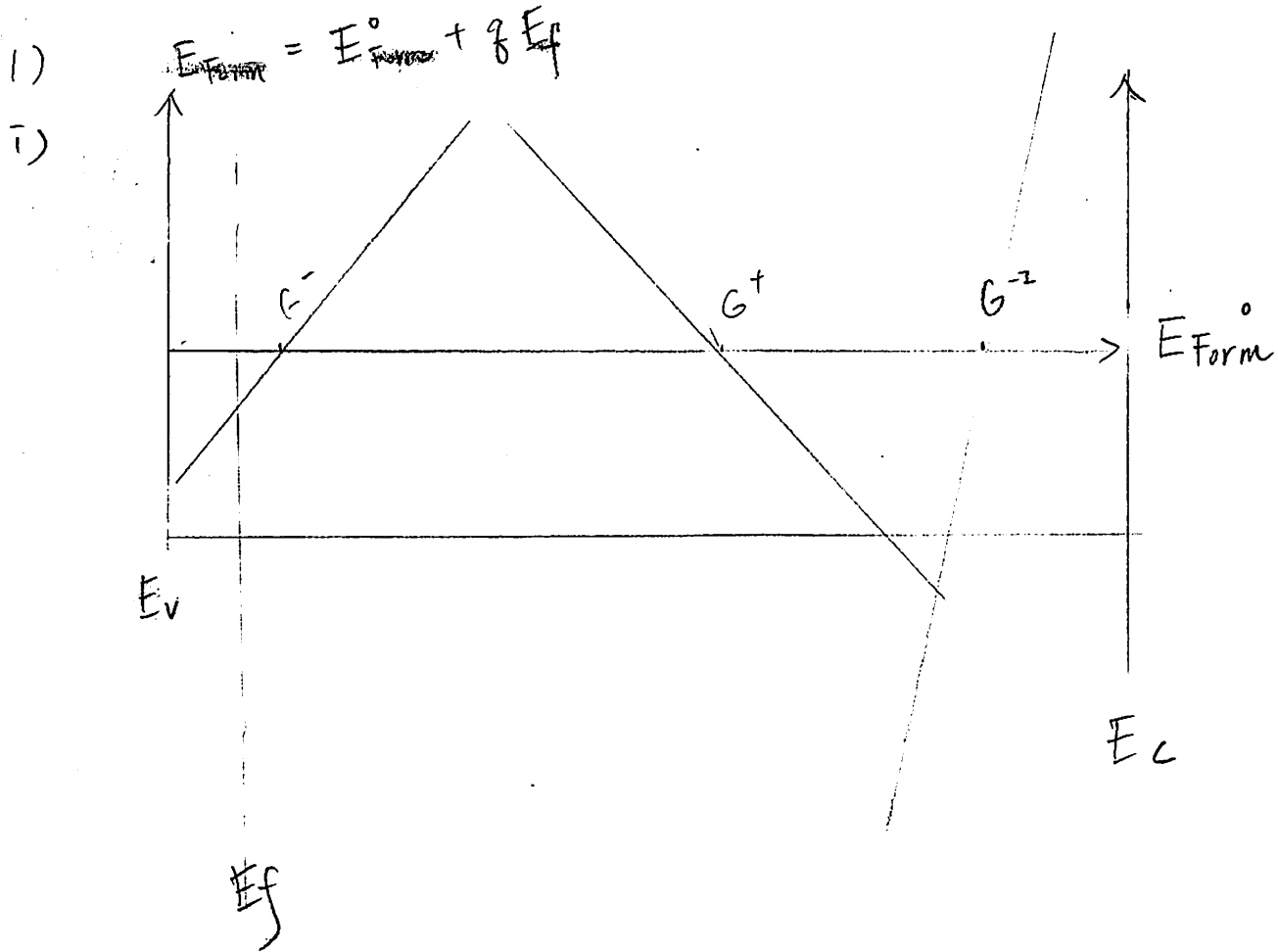
Here I found on the semiconductor today's example is quantum cascade laser (QCL). The first QCL experiment is conducted by Jerome Faist, Federico Capasso and the well-known co-inventor of MBE Alfred Cho in 1994. The first QCL was based AlInAs/GaInAs QWs on InP substrate. Within 20 years, QCL has been improved from cryogenic temperature to room temperature operation, and can reach power as high as Watt level.

The article is published at Applied Physics Letter, "High power Sb-free quantum cascade laser emitting at $3.3\mu\text{m}$ above 350K", written by A. Bismuto, M. Beck and J. Faist. Their device active region consists of $\text{In}_{0.72}\text{Ga}_{0.28}\text{As}$, $\text{In}_{0.52}\text{Al}_{0.48}\text{As}$ and AlAs quantum well structures. Their uniqueness is that usually QCL's emission wavelength under $3.6\mu\text{m}$ needs to incorporate Sb into the structure, but this material is not allowed for commercial users. Their new design can achieve comparable output power with Sb-based QCL. Generally, in order to make high efficiency QCL, researcher needs to design the injection and extraction superlattices in the device, here they used bound to continuum design. Composite binary alloys are suitable for this kind of application. They can achieve low threshold current of $3.6\text{kA}/\text{cm}^2$ and slope efficiency of $600\text{mW}/\text{A}$. And the laser can work at room temperature.



Right hand side is their active region design. Left hand side is the Power vs current curve.

Problem 4.4)

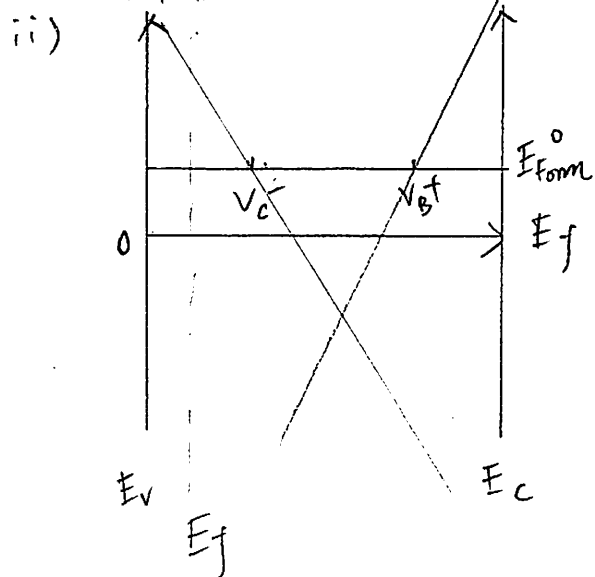


The charge state with the minimum formation energy should be the dominant state in the crystal. And

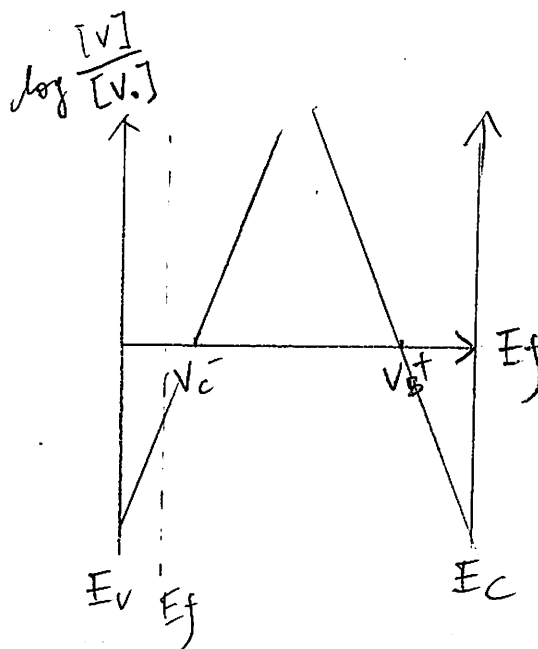
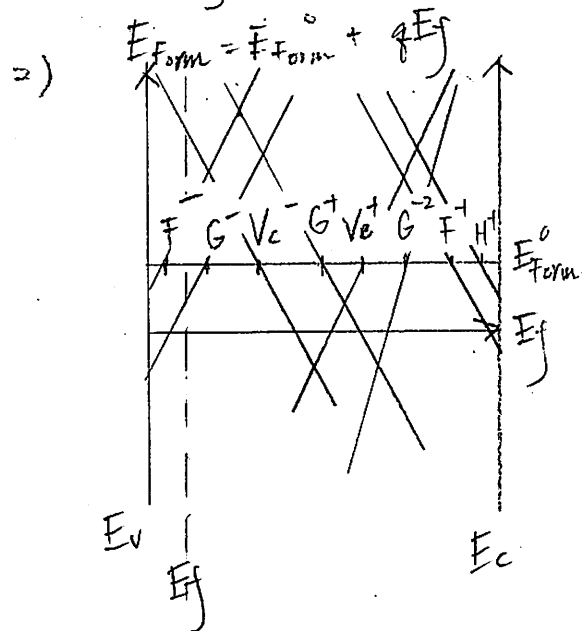
G is a group I atom, which means doping this into III-V semiconductor should give us p-type crystal. So E_f should be near the valence band. As we can see from the above figure, G^{2-} state gives us the minimum energy. Therefore, G^{2-} state is the majority.

Problem 4.4)

i) $E_{\text{Form}} = E_{\text{Form}}^0 + qE_f$

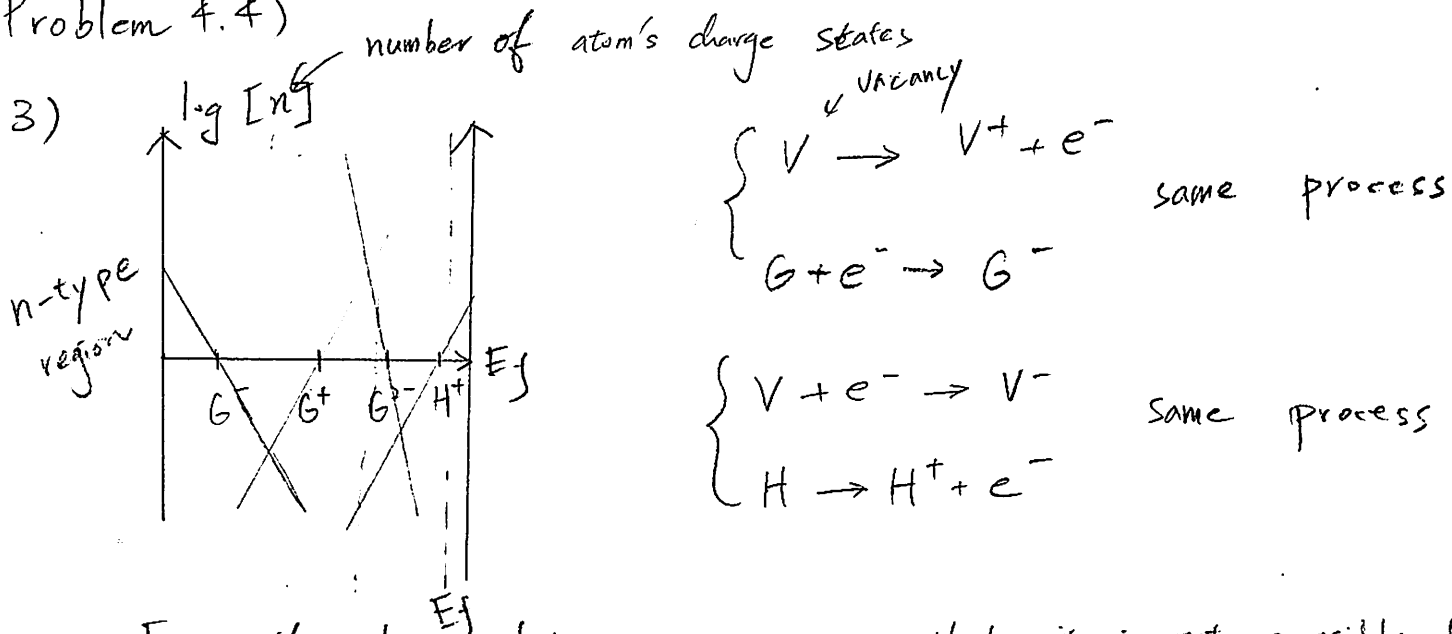


The minimum formation energy occurs for V_B^+ state. Therefore, the majority is V_B^+ .



From the argument in Sec. 7.1.5, we can draw number of charged states as left hand side. And we know for G atom doping is p-type. Fermi level should be near the valence band. We can see that the intersection with E_f is higher for V_B^+ state, which means V_B^+ vacancy will dominate.

Problem 4.4)



From the above plot, we can see that it is not possible for G atom to make huge influence on n-type side.

As we can see from the figure, E_f is near conduction band for n-type semiconductor. Even if there are some G atoms in this region, the preferred state is G^+ state.

Hence, G atoms in n-type region wouldn't be trapped centers.

4) a. So F atom acts as an acceptor in the crystal.

The electron negativity of F is higher than C , which means it would grab electrons more strongly than original C atoms in the semiconductor. Hence, F atoms will replace C atoms.

b. To determine whether F will segregate or not, we need to discuss the diffusivity. From Eq. (7.10) in Rockett's book, we have

$$D_F = D_{q=0} + D_{+1} \left(\frac{P}{n_i} \right)$$

$$D_G = D_{q=0} + D_{+1} \left(\frac{P}{n_i} \right) + D_{+2} \left(\frac{P}{n_i} \right)^2$$

Problem 4.4)

4) b. From the above two equations, we can see that diffusivity

of G has second order dependence on doping concentration.

Therefore, if all the other parameters are the same, G atoms have larger diffusivity. It is more likely for G to segregate to the surface than F atom.

c. If we want to use an atom as surfactant, the atom should have the ability to passivate dangling bonds at surface.

Generally, these materials segregate strongly to the surface.

Therefore, it's more likely to choose G atom as surfactant.

5)

a. no G atoms. \Rightarrow only H atoms contributes as donors.

$$E_F - E_i = k_B T \ln \left(\frac{N_d}{n_i} \right)$$

$$E_F \approx 1.245 \text{ eV above valence band.}$$

b.

$$[G^-] / [G_0] = e^{\frac{E_f - E_{G^-}}{k_B T}} \approx 2.51 \times 10^{18}$$

$$E_f - E_{G^-} = 1.09 \text{ eV}$$

$$c. [G^{-2}] / [G^-] = e^{\frac{E_f - E_{G^{-2}}}{k_B T}} \approx 275$$

Problem 4.4)

5.) d. $[G_{total}] = [G_0] + [G^-] + [G^{2-}] = 9.8 \times 10^{16}$

$$= [G_0] (1 + 1.28 \times 10^{18} + 1.28 \times 10^{18} \times 140) = 9.8 \times 10^{16}$$

$$[G_0] = 1.4 \times 10^{-4} \text{ cm}^{-3}$$

$$[G^-] = [G_0] \cdot 1.28 \times 10^{18} = 3.52 \times 10^{14} \text{ cm}^{-3}$$

$$[G^{2-}] = [G^-] \cdot 140 = 9.69 \times 10^{16} \text{ cm}^{-3}$$

e.

$$E_F - E_i = k_B T \ln \left(\frac{N_d - N_a}{n_i} \right) \quad N_a \approx [G^{2-}]$$

$$\Rightarrow E_F \approx 1.1558 \text{ eV}$$

$$\text{Error} \Rightarrow 1.245 - 1.228 \approx 0.089 \text{ eV}$$

6)

$$N = 5 \times 10^{22} \text{ cm}^{-3} \quad T = 400 \text{ K}$$

$$E_{VB} = 2 \text{ eV}, \quad E_F = 1.25 \text{ eV}$$

$$[V_B^0] = N e^{-\frac{E_{VB}}{k_B T}} = 5 \times 10^{22} \cdot e^{-\frac{2}{k_B T}} = 3.155 \times 10^{11} \text{ cm}^{-3}$$

$$[V_B^+] = [V_B^0] \cdot e^{-\frac{(E_F - E_i + 1)}{k_B T}} \approx 1.043 \times 10^{13} \text{ cm}^{-3}$$

$$[V_C^0] = N e^{-\frac{E_{VC}}{k_B T}} = 1.93 \times 10^5 \text{ cm}^{-3}$$

$$[V_C^-] = [V_C^0] e^{-\frac{(E_F - E_i)}{k_B T}} = 2.39 \times 10^{10} \text{ cm}^{-3}$$

↑

majority as expected.

Problem 4.5)

$$7) \quad a_{\text{GaInAs}} = 0.572 \text{ nm}$$

$$a_{\text{GaAs}} = 0.565 \text{ nm}$$

$$a_{\text{InP}} = 0.587 \text{ nm}$$

$$f = \frac{a_s - a_f}{a_f}$$

$$f_{\text{GaInAs/GaAs}} = \frac{0.565 - 0.572}{0.565} = -0.0124$$

$$f_{\text{GaInAs/InP}} = \frac{0.587 - 0.572}{0.587} = 0.0256$$

8)

$$\alpha = 1$$

$$\nu = 0.29$$

$$\theta = \phi = 60^\circ$$

From Eq. 7.30 in Rockett, we have

$$\frac{\frac{hc}{b}}{\ln\left(\frac{\alpha hc}{b}\right)} = \frac{1 - \nu \cos^2 \theta}{8\pi f (1 + \nu) \cos \phi}$$

To look for solution, I used Mathematica to get numerical value.

$$\Rightarrow \frac{hc}{b} \approx 11.13$$

9) As we increase the film thickness above critical thickness, the strain energy in the film will exceed the formation energy of dislocation, which means film will tend to form dislocation in order to minimize the energy. Introduction of dislocations into the interface can decrease the effective misfit in the film and substrate.

Problem 4.5)

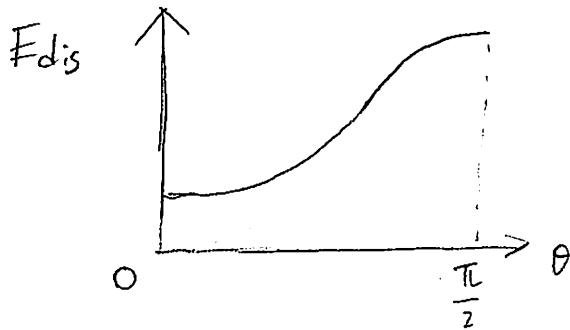
10)

$$a. \quad E_{dis} = \frac{Gb^2}{4\pi} \frac{1 - \nu \cos^2 \theta}{1 - \nu} \ln\left(\frac{\alpha h}{b}\right)$$

Case (1) Perfect edge dislocation $\Rightarrow \theta = 0 \Rightarrow \cos^2 \theta = 1$

Case (2) 60° partial dislocation $\Rightarrow \theta = 60^\circ \Rightarrow \cos^2 \theta = \frac{1}{4}$

Case (3) Perfect screw dislocation $\Rightarrow \theta = 90^\circ \Rightarrow \cos^2 \theta = 0$



To give the maximum strain relief, we need the largest E_{dis} , which is the Case 3. perfect screw dislocation.

b. The most likely to form is the one with the minimum E_{dis} , which is the perfect edge dislocation.

11)

$$N_d = 1.1 \times 10^{15} \text{ cm}^{-3}$$

From Fig. 7.26 in Rockett, we can get an approximation of the radius of dislocation effects on carrier. Assume \vec{b} and dislocation line are perpendicular. $\Rightarrow \alpha = \frac{\pi}{2}$

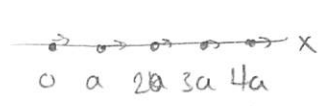
$$\pi^2 R N_d = \frac{f \sin \alpha}{a} \Rightarrow R = \sqrt{\frac{f}{a \pi N_d}}$$

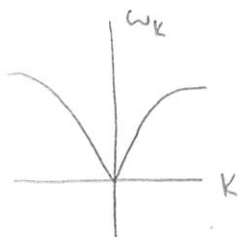
$$\approx 7.1 \times 10^{-5} \text{ cm}$$

$f = 1$ here.

#

4.1)

a. In a 1D crystal, something like  There will be acoustic phonons, and the dispersion relation will look like:




because there is one atom basis. Right at $k=0$ there is a zero-energy mode called a Goldstone mode that corresponds with the overall translation of the whole system.

More generally, this and other Goldstone modes arise from a broken continuous symmetry. In the case of phonons, the continuous symmetry is translational, i.e. you can move the system in the x direction and everything looks exactly the same. These modes necessarily have 0 energy because the symmetry of space (translational) means that there is no preferred direction in which the system has higher or lower energy.

In a perfect semiconductor crystal, in 3 dimensions, there could be more of these modes, one for each continuous symmetry broken. This amounts to "phonons" that represent the overall translation of the crystal in any of 3 directions.

b. For the 1D case: there is only 1 dimension, so $\vec{q} = (k_{out} - k_{in})\hat{x}$, and

 $S(q) = \frac{1}{N} \left| \sum_{j=0}^{N-1} e^{iqR_j} \right|^2$, $R_j = aj$ defines the lattice points

$$\sum_{j=0}^{N-1} e^{iqaj} = \sum_{j=0}^{N-1} (e^{iqa})^j = \text{geometric series} = \frac{1 - e^{iqaN}}{1 - e^{iqa}} = \frac{e^{iqaN/2} (e^{-iqaN/2} - e^{iqaN/2})}{e^{iqa/2} (e^{-iqa/2} - e^{iqa/2})}$$

$$= \frac{e^{iqaN/2}}{e^{iqa/2}} \frac{(2i) \sin(qaN/2)}{(-2i) \sin(qa/2)} \quad \text{so, taking the mag:}$$

$$S(q) = \frac{1}{N} \frac{\sin^2(Naq/2)}{\sin^2(aq/2)} = | \dots |^2$$

c. A plot of this for $N=10$, $0 \leq qa \leq 10\pi$ is attached. From counting, there are 8 small peaks between each maxima, not counting the maxima.

A plot with $N=100$ is also attached, now the maximum peaks have amplitude 100.

In general, maxima happen when $Naq/2 = n\pi$ and $aq/2 = m\pi$, where $n, m = 0, \pm 1, \pm 2, \dots$

We need both to be satisfied, so: $\frac{aq}{2} = \frac{n}{N}\pi = m\pi$

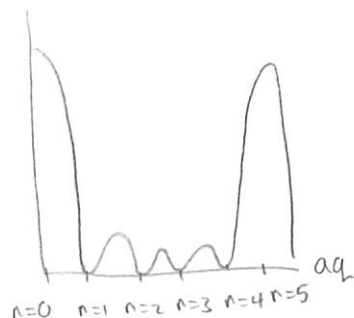
Under this condition, $n = Nm$, so: $S(q) = \frac{1}{N} \frac{\sin^2 Nm\pi}{\sin^2 m\pi} = \lim_{m \rightarrow 0} \frac{1}{N} \frac{\sin^2(Nm\pi)}{\sin^2(m\pi)}$

$$= \frac{1}{N} \lim_{m \rightarrow 0} \frac{2\pi \cos Nm\pi \sin Nm\pi}{2\pi \cos m\pi \sin m\pi} = \lim_{m \rightarrow 0} \frac{(-N \sin^2 Nm\pi + N \cos^2 Nm\pi)\pi}{(\sin^2 m\pi + \cos^2 m\pi)\pi} = \boxed{N}$$

So the maximum peak has amplitude N .

The zeros in between the maxima comes when the numerator is 0:

$$\sin\left(\frac{Naq}{2}\right) = 0 \Rightarrow \frac{Naq}{2} = n\pi$$



The large peaks come when the denominator = 0, like before,

so $\frac{aq}{2} = m\pi \Rightarrow aq = 2\pi m$ is the separation of maxima

→ the separation of minima is $aq = \frac{2\pi}{N}$

So from one maximum to the other there are $\frac{2\pi}{\frac{2\pi}{N}} = N$ minima, including the 2 maximum peaks themselves, which happen also when the numerator = 0.

So in each period there are N minima, but one corresponds with the main peak so there are really $n-1$ true minima. Then $N-1$ minima means $N-2$ maxima, so in total there will be $\boxed{N-2}$ satellite peaks, not including the maximum peaks.

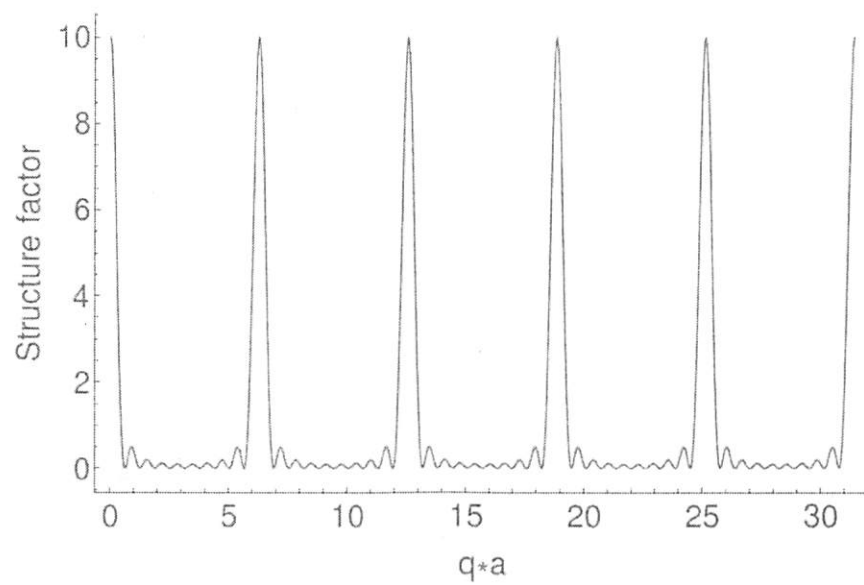
d. Plots of $S(q)$ for $N=10$ and $N=100$ are attached, each with 3 randomly missing atoms.

For $N=10$, the maximum peak height is ~ 5 , which is much smaller than the 10 it started with. Also, now there are 4 smaller peaks between the main peaks, but they are poorly defined.

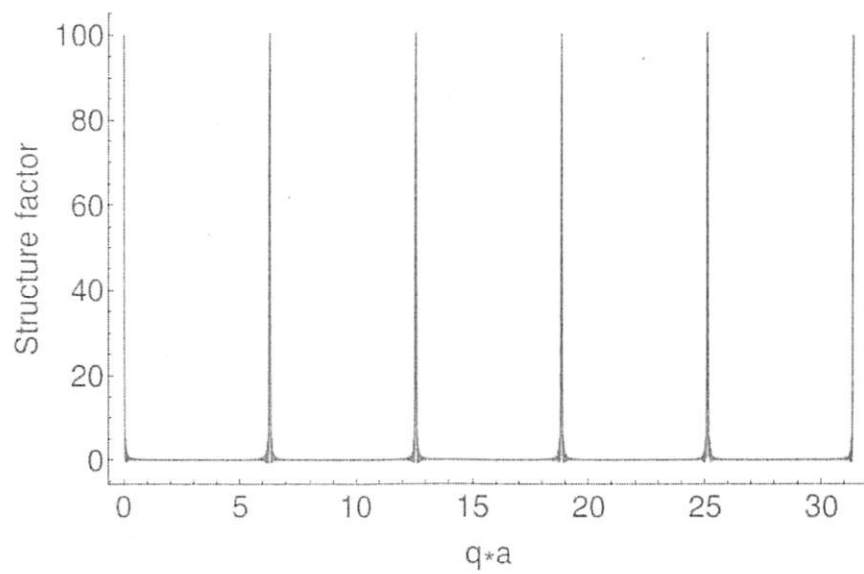
For $N=100$, the new peak height is around 95, As only 3/100 atoms were removed, this did not have such a large effect. The width is hard to estimate, but it seems to be about $0.05 = \Delta(qa)$ which is similar to the case with no defects.

In general, diffraction experiments would not be so useful to get information about point defects because the pattern is not so sensitive to defects if they have a fairly low density, (as they normally do). Furthermore, even if they have a high density as in the first case, the diffraction pattern contains very little information about the location of defects, although maybe you can extract some information about the # of defects.

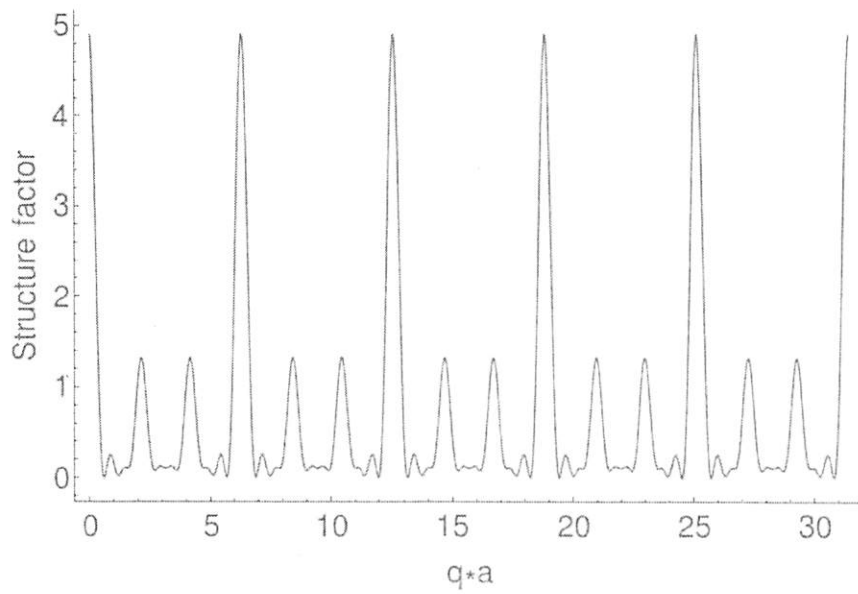
$\frac{2\pi}{2\pi}$



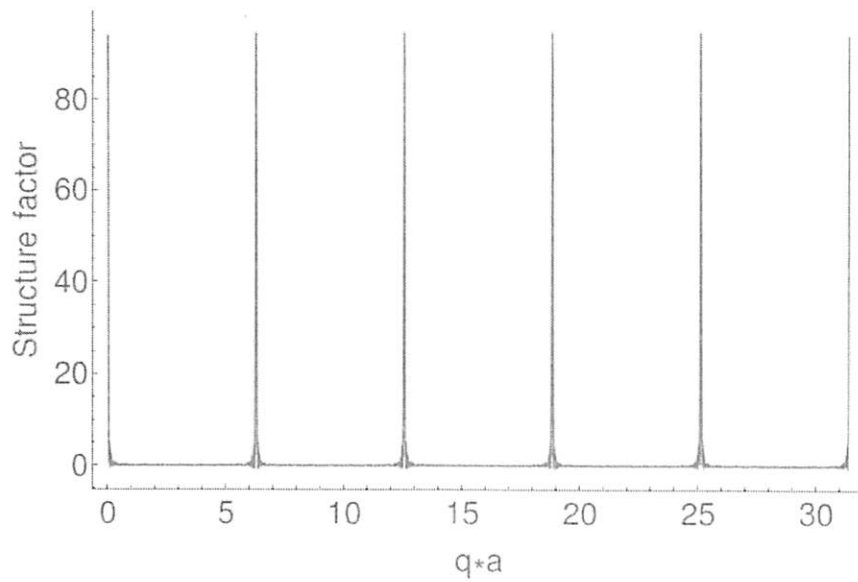
4.1c: Structure factor for a linear crystal with $N = 10$.



4.1c: Structure factor for a linear crystal with $N = 100$.



4.1d: Structure factor for a linear crystal with $N = 10$ but three random sites missing.



4.1d: Structure factor for a linear crystal with $N = 100$ but three random sites missing.

4.2) a. At $T=0$, there should be no displacement, so $S(\vec{q}, T=0) = \frac{1}{N} \left| \sum_{j=1}^N e^{i\vec{q} \cdot \vec{R}_j} \right|^2$

$$= \frac{1}{N} \sum_j e^{i\vec{q} \cdot \vec{R}_j} \sum_k e^{-i\vec{q} \cdot \vec{R}_k} = \frac{1}{N} \exp \left\{ \sum_j \sum_k i\vec{q} \cdot (\vec{R}_j - \vec{R}_k) \right\}$$

With the mapping $\vec{R}_i \rightarrow \vec{R}_i + \vec{u}_i(t)$, $S(\vec{q}, T) = \frac{1}{N} \sum_j e^{i\vec{q} \cdot \vec{R}_j + i\vec{q} \cdot \vec{u}_j(t)} \sum_k e^{-i\vec{q} \cdot \vec{R}_k - i\vec{q} \cdot \vec{u}_k(t)}$

Now $u_i(t)$ fluctuates, but it fluctuates randomly, so we will be interested in some kind of average of the second term $\langle e^{i\vec{q} \cdot \vec{u}_j(t)} \rangle$.

This gives $S(\vec{q}, T) = \frac{1}{N} \sum_j e^{i\vec{q} \cdot \vec{R}_j} \langle e^{i\vec{q} \cdot \vec{u}_j} \rangle \sum_k e^{-i\vec{q} \cdot \vec{R}_k} \langle e^{-i\vec{q} \cdot \vec{u}_k} \rangle$

These averages are the same for every atom, because the thermal motion is random, so we can take them out of the sums:

$$S(\vec{q}, T) = \left[\frac{1}{N} \sum_j e^{i\vec{q} \cdot \vec{R}_j} \sum_k e^{-i\vec{q} \cdot \vec{R}_k} \right] \langle e^{i\vec{q} \cdot \vec{u}} \rangle \langle e^{-i\vec{q} \cdot \vec{u}} \rangle = S(\vec{q}, T=0) \langle e^{i\vec{q} \cdot \vec{u}} \rangle \langle e^{-i\vec{q} \cdot \vec{u}} \rangle$$

This is not quite what the sheet has but everything works out in the end. ✓

b. We will be expanding $\langle e^{i\vec{q} \cdot \vec{u}} \rangle$ using a Taylor Series:

$$\langle e^{i\vec{q} \cdot \vec{u}} \rangle = \left\langle 1 + i\vec{q} \cdot \vec{u} + \frac{(i\vec{q} \cdot \vec{u})^2}{2} + \dots \right\rangle = 1 + i\vec{q} \cdot \langle \vec{u} \rangle - \frac{\langle (\vec{q} \cdot \vec{u})^2 \rangle}{2} + \dots$$

This is useful because $\vec{q} \cdot \vec{u}$ on average is 0, there is no preferred direction.

This means we can approximate $\langle e^{i\vec{q} \cdot \vec{u}} \rangle \approx 1 - \frac{\langle (\vec{q} \cdot \vec{u})^2 \rangle}{2}$, but in general

$$e^x = 1 + x, \text{ so now } \langle e^{i\vec{q} \cdot \vec{u}} \rangle \approx e^{-\langle (\vec{q} \cdot \vec{u})^2 \rangle / 2} = e^{-q^2 \langle |\vec{u}|^2 \rangle / 2}$$

For atoms vibrating because of thermal noise, they approximately look harmonic, so $E = \frac{1}{2} k u^2$, where k is the spring constant, In terms of ω , and M ,

$$k = \omega_0^2 M, \text{ so } E = \frac{1}{2} M \omega_0^2 u^2, \text{ and } \langle E \rangle = \frac{1}{2} M \omega_0^2 \langle |\vec{u}|^2 \rangle$$

$$\text{From thermodynamics, } \langle E \rangle = \frac{1}{2} k_B T, \text{ so now } \langle |\vec{u}|^2 \rangle = \frac{k_B T}{M \omega_0^2}$$

and so $\langle e^{i\vec{q} \cdot \vec{u}} \rangle = e^{-q^2 k_B T / 2 M \omega_0^2}$. Finally, plugging this in:

$$S(\vec{q}, T) = S(\vec{q}, T=0) e^{-q^2 k_B T / 2 M \omega_0^2} e^{-q^2 k_B T / 2 M \omega_0^2} = S(\vec{q}, T=0) e^{-q^2 k_B T / M \omega_0^2}$$

c. With this structure factor, the first term $S(\vec{q}, T=0)$ will be the same as before, so

$$S(\vec{q}, T) = \frac{1}{N} \frac{\sin^2\left(\frac{Naq}{2}\right)}{\sin^2\left(\frac{aq}{2}\right)} e^{-\left(\frac{K_B T q^2}{M\omega_0^2}\right)}$$

Whereas before the higher order peaks all had the same amplitude, now the spectrum falls off like a gaussian because of the $e^{-K_B T q^2 / M\omega_0^2}$ term. This makes sense because higher q corresponds to higher frequency x-rays that fit more wavelengths between each atom.

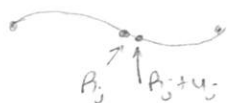
If each atom is displaced a little, the phase of light can change



classically. This means the light will see low order even if the atoms only move a small distance from A_j .

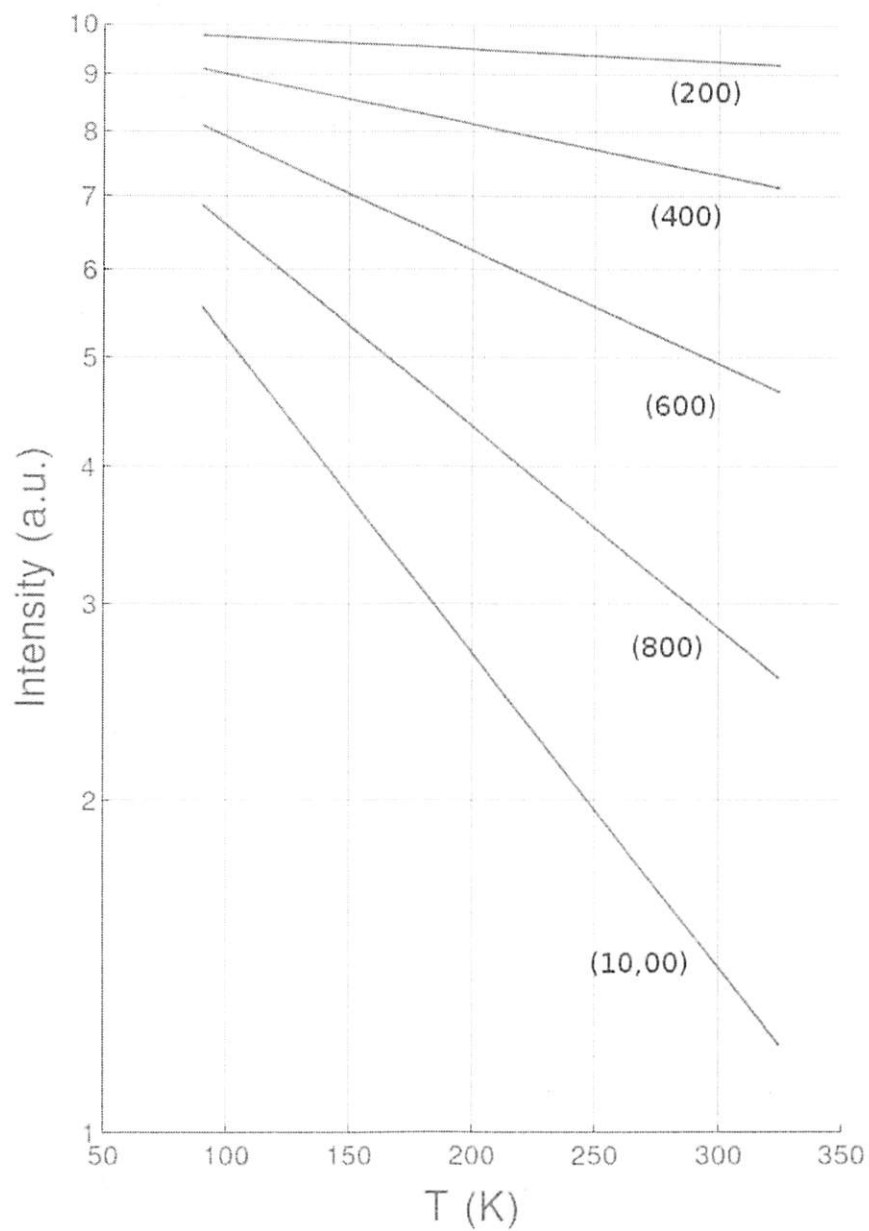
At longer wavelengths, the light is less susceptible to small changes in A_j .

So the structure factor remains approx. the same.



d. A plot of the peak intensity of the (200), (400), (600), (800), and (10,00) peaks is attached. The parameters used to get the peaks are $n=10$, $M=27 \text{ mp}$, $\omega_0=0.34 \times 10^{14} \text{ rad/sec}$, $a=0.4 \text{ nm}$. As expected, and shown in $S(\vec{q}, T) = S(\vec{q}, 0) e^{-\left(\frac{K_B T q^2}{M\omega_0^2}\right)}$, for the peaks at higher q the finite temperature has a larger effect. Furthermore, the temperature dependence is exponential which shows up as a line on the log scale plot. Quantitatively, the values compare decently well to the experimental data in Figure 1, and in particular the relationship is a straight line on the log plot which indicates exponential dependence. The agreement is not as good for low T , as presumably other factors become more important.

e. The higher- q peaks show a strong temperature dependence, so in this sense measuring their relative amplitudes could effectively measure the temperature. Of course it requires calibrating because it could be hard to get ω_0 , but that would not be too much of an issue. This would work best first of all for semiconductors with fairly small ω_0 , or equivalently small "spring constants" between the atoms, as that would increase the effect T would have on the intensities. It also requires a very pure crystal, so that the peaks are not reduced so much from defects and the temperature dependence can be seen most clearly. Finally, for the same reason as ω_0 , this would work best for crystals with small M .



4.2d: Diffraction peak intensity as a function of temperature, for the (200), (400), (600), (800), and (10,00) peaks. The parameters used for this are $M=27\text{ mp}$, $w_0=0.34 \times 10^{14} \text{ rad/sec}$, $a=0.4 \text{ nm}$.

4.3) a. In general there are 5 types of cells in a lattice of a III-V ternary alloy, such as $\text{In}_{1-x}\text{Ga}_x\text{As}$. In each the center atom is As, and there are 0, 1, 2, 3 or 4 Ga atoms and 4, 3, 2, 1, and 0 In atoms bonded to it. At any given composition there will be a different number of cells of each type. The # of cells of type i is given by

$N \alpha_i q_i$, where N is the number of atoms total, α_i is the degeneracy of configuration i , and q_i is the probability that configuration i appears. The degeneracy is needed because while there is only 1 way to form a type 0 cell there are 6 unique ways to form type 2 cells.

We want to find the ratio of cells of type i , so $\frac{N \alpha_i q_i}{N} = \alpha_i q_i$, which amounts to finding q_i . If the atoms are distributed randomly, with no structure, then q_i depends only on x , as the composition determines the most likely cell types. In this case, $q_i = x^{4-i} (1-x)^i$, and this is used to plot $\alpha_i q_i$ for each i as a function of composition, in Figure 3 as the dotted line.

The atoms are really not distributed randomly, however, because each crystal cell type feels a different amount of strain at different concentrations due to bond stretching and bond bending. This is modelled by assuming that at any x , the atoms lie on the planes of a virtual crystal, with lattice constant linearly interpolated from that of GaAs to that of InAs based on x . Each cell type has bonds that stretch different amounts, so each cell type has a different strain energy at a given x . This strain energy is shown in Figure 2 in the paper, and used for later calculations.

To find the true cell ratios, the strain needs to be taken into account by writing a free energy function that takes into account the strain mixing enthalpy, and the entropy associated with mixing:

$$F = N \sum_i \alpha_i q_i \epsilon_i - N k_B T (3[x \ln x + (1-x) \ln(1-x)] - \sum_i \alpha_i q_i \ln q_i)$$

To find the equilibrium q_i values, F must be minimized. In the paper they use

the method of Lagrange multipliers and obtain $q_i = c \eta_i + 4-i$, where c is the normalization constant $c = \left(\sum_i \eta_i + 4-i \right)^{-1}$, η_i comes from the strain: $\eta_i = e^{-\epsilon_i/kT}$

and $+$ is the positive solution to $(1-x)\eta_0^4 + (3-4x)\eta_1^3 + (3-6x)\eta_2^2 + (1-4x)\eta_3 + -x\eta_4 = 0$.

This solution comes from a system of equations. 5 of the equations come from the Lagrange multipliers form: (for each i)

$$\frac{\partial F}{\partial q_i} + a z_i + b \gamma_i = 0, \text{ where } a \text{ and } b \text{ are the Lagrange multipliers and}$$

$$z_0=1, z_1=3, z_2=3, z_4=1, z_5=0.$$

The other two equations are normalization: $\sum_i \alpha_i q_i = 1$, and the constraint on the composition $x = q_0 + 3q_1 + 3q_2 + q_3$.

The 7 unknowns are q_0, q_1, q_2, q_3, q_4 , and a and b . Solving this system gives the solution above.

These q_i 's are used to plot the dark solid line in Figure 3, by ratio of cell $i = q_i / \alpha_i$, at each x . Generally these depend on temperature, and in this case

$$T = 1000 \text{ K.}$$

A reproduced Figure 3 is attached, showing the ratio of cell, $\alpha_i q_i$, as a function of x for each cell. The solid line corresponds to q_i 's derived from the thermodynamics and the dashed line corresponds to q_i 's derived from combinatorics and statistics. It shows the amount of each cell in a crystal made up of a given composition.

Next, the short range order parameter β is defined as $\beta = 1 - P_{ab}/x$, where P_{ab} is the probability that G_a is a second nearest neighbor with I_n . By counting cells, this comes out to be $\beta = 1 - \frac{q_1 + 2q_2 + q_3}{x(1-x)}$, and this is plotted in Figure 4 with the q_i 's derived from the thermodynamics derivation, as a function of x at $T = 2000 \text{ K, } 1000 \text{ K, and } 500 \text{ K,}$

The order parameter β effectively measures the tendency for atoms to alternate G_a , then I_n , in which case β is negative. Therefore $\beta < 0$ implies some short range order and $\beta > 0$ implies some clustering. In Figure 4, that $\beta < 0$ always indicates that in $G_a A_3$ there tends to be short range order, instead of clustering. Furthermore, as T decreases β decreases, indicating more order. This makes sense as at lower temperatures there should be more order.

A reproduced Figure 4 is attached.

Finally, this same information is plotted in Figure 5, but now the temperature dependence is emphasized. All of the information is for $x=0.5$, so $\text{In}_{0.5}\text{Ga}_{0.5}\text{As}$.

First, the order parameter β is shown as a dashed line, and the values are shown on the left. As expected, at lower T the crystal becomes more ordered, but it flattens out at $\beta = -1/3$.

The ratio of cell is also shown for $x=0.5$ as solid lines, one for each type, and the values are on the right. At low temperatures the strain enthalpy dominates and type 2, with the strain energy at $x=0.5$, dominates. At higher temperatures entropy becomes important and eventually dominates.

A reproduced Figure 5 is attached.

b. The major point this paper presents is that through a thermodynamic argument considering the strain enthalpy and mixing entropy, III-V compound semiconductors prefer to order instead of cluster over a short range.

The clustering argument makes intuitive sense: in general the total strain energy can be minimized if instead of lying in planes of a virtual crystal, the atoms cluster into like regions where the strain can relax. This is further supported by the evidence that clustering like this occurs on a macroscopic scale. What the authors shows however, is that this clustering is not what happens on a microscopic scale. Instead it is energetically preferable overall for there to be some short range order, instead of clustering. This can be understood as microscopically, the energy cost of forming clusters overall is higher than order because of the interactions near the edges of the clusters.

good! $\frac{20}{20}$

C. This paper discussed III-V ternary alloys in general, but used InGaAs for all of the examples. From 'Semiconductor Today,' examples of recent applications of InGaAs that people are interested in include quantum wells for quantum information processing, high speed photodetectors, and high quality MOSFETs. In each of these InGaAs is the active material, and therefore understanding the microscopic ordering and the effect of strain is important to optimize the material for applications.

At the end of 2015 Bechtold et al (*Nature Physics*, 11, 1005-1008 (2015)) used InGaAs quantum dots on GaAs to study trapped single electrons, and in particular the mechanisms of loss of quantum information. One of the mechanisms they identified, in fact, was strain that creates electric fields on a microscopic scale. By using a (strong) magnetic field, they were able to reduce the effect of this and other loss mechanisms, and increase the lifetime of quantum information. They present this research as a step towards InGaAs-based quantum computers.

Near the middle of 2015, Semiconductor Today reported that Marktech launched a high speed photodetector using InGaAs. The photodetectors operate from 0.9-1.7 μm , which is good for optical communications. They claim that the photodetectors can support high data rates and low dark current, increasing the signal to noise ratio.

Finally, at the beginning of 2015 Kim et al (*IEEE Electron Device Letters*, (2015)) demonstrated an InGaAs MOSFET with a good sub-threshold swing, transconductance, and on-current. The device was made with InGaAs and InP, with an InGaAs channel. The devices were grown with MBE.

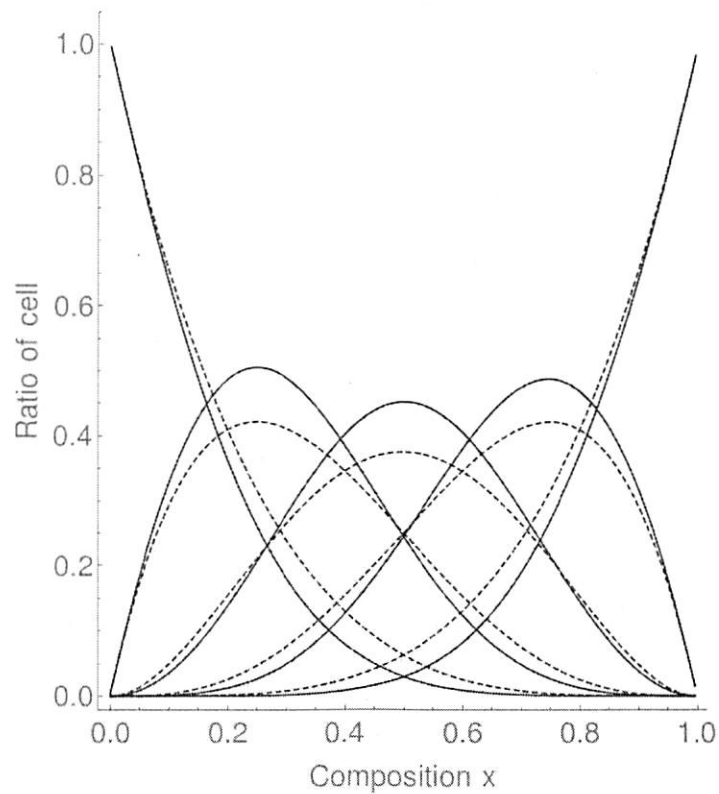


Figure 3: Ratio of cell as a function of composition. The solid line is calculated taking into account strain energy and entropy at 1000 K, the dashed line is calculated assuming the atoms are distributed at random.

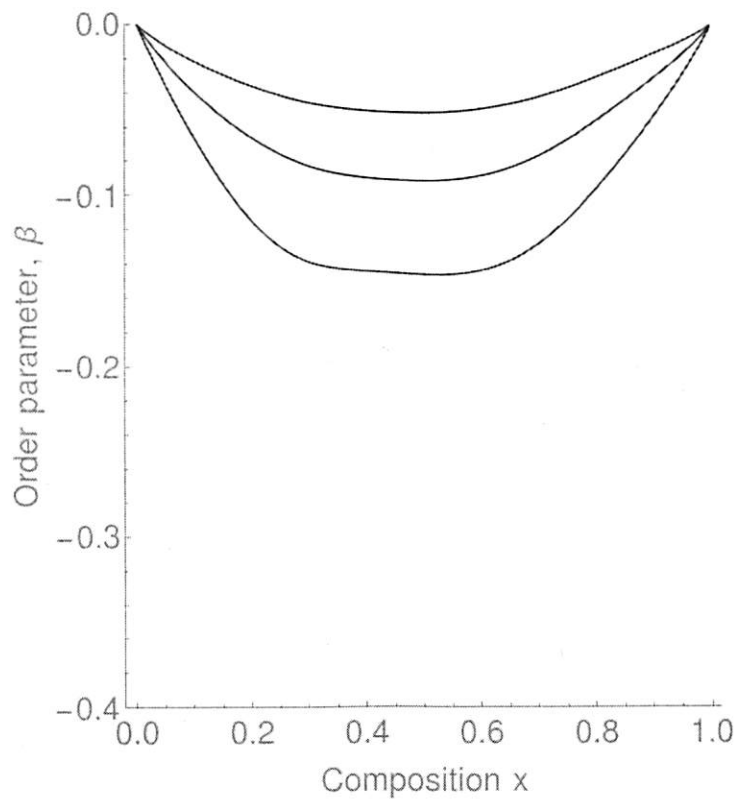


Figure 4: Order parameter as a function of composition. From top to bottom, the lines are calculated for 2000 K, 1000K, and 500 K.

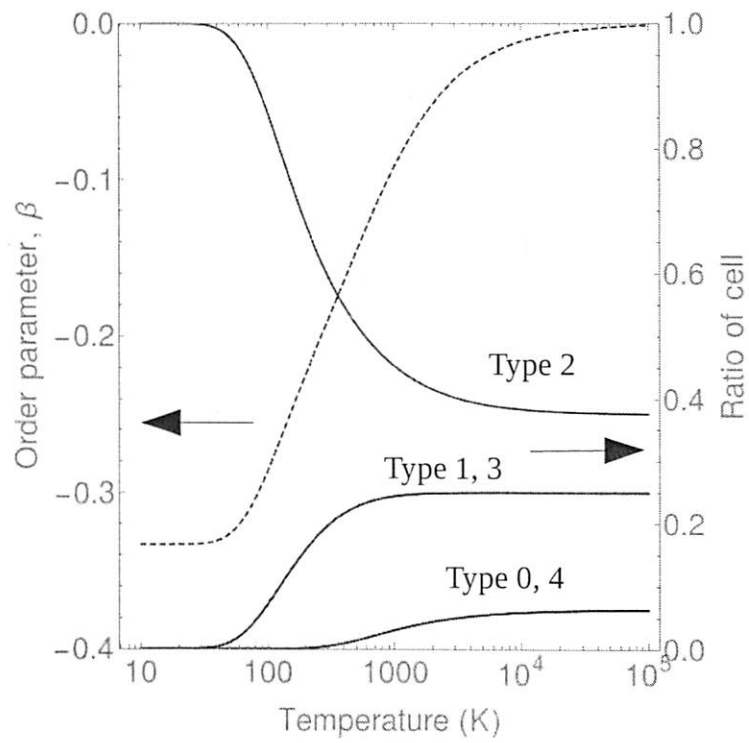


Figure 5: Order parameter and ratio of cell as a function of temperature, for $x = 0.5$. The dotted line is the order parameter and the solid lines are the ratio of cell for each type of cell.

4.4) 1. G is an acceptor because it is in group I, so it will pull down the Fermi level to around the shallow level for G^- .

i. Most of the G atoms will be in the -1 state, as the Fermi energy will be slightly above G^- so electrons will tend to ionize G atoms once.

ii. V_c vacancies will be neutral as they are too deep and will therefore not be ionized.

V_R vacancies will be charged $+1$ as the Fermi level is below their energy, so they will not be neutralized.

2. V_R vacancies will be more common when the material is doped with G (acceptors). The uncharged vacancy concentration generally does not change too much with Fermi level, but at the same time

$$\frac{[V_R^+]}{[V_R]} = e^{-(E_F - E_{+1})/kT} \quad , \quad \frac{[V_c^-]}{[V_c]} = e^{-(E_F - E_-)/kT}$$

E_F is close to the valence band, so $[V_R^+]$ will be very high while $[V_c^-]$ will be very small. While there may not be very many neutral vacancies, then, there will be many charged V_R vacancies.

3. On the n side, doped heavily with H, the Fermi level will be close to the conduction band, so any residual G atoms will be in the G^{2-} state. Most likely, these will act as traps, because doubly charged ions are often traps as they can take a minority carrier (hole), while still repelling e^- because the charge is now -1 .

4. a. If F is an acceptor, then it must replace the group V atom B primarily. In that case there would be 1 less electron than before, making it an acceptor.

b. F would have a greater tendency to go to the surface because it has a larger radius than G, and the larger atom wants to minimize its strain energy more, which can happen on the surface.

c. F would be more likely to work as a surfactant because it has a larger size, so it would go to the surface, and also it is one group away from the III-V lattice, which is desirable.

5. a. If there are no G atoms, $N_a = 0$, $N_d = 2 \times 10^{17} \text{ cm}^{-3}$, so

$$E_f = E_i + kT \ln \left(\frac{N_d}{n_i} \right) = \boxed{1.24 \text{ eV}} \text{ from valence band}$$

b. $\frac{[G^-]}{[G_0]} = e^{(E_f - E_{G_0})/kT}$, $E_{G_0} = 0.15 \text{ eV}$ from valence band, so $\frac{[G^-]}{[G_0]} = \boxed{2.6 \times 10^{18}}$

c. $\frac{[G^{2-}]}{[G^{-1}]} = e^{(E_f - E_{G_2})/kT} = \boxed{232}$

d. There will be basically no neutral G atoms, to good approximation, so

$$[G^{2-}] + [G^{-1}] = 9.8 \times 10^{16} \text{ cm}^{-3}, \quad \frac{[G^{2-}]}{[G^{-1}]} = 232$$

$$\Rightarrow [G^{-1}](1 + 232) = 9.8 \times 10^{16} \text{ cm}^{-3} \Rightarrow \boxed{[G^{-1}] = 4.21 \times 10^{14} \text{ cm}^{-3}}$$

$$[G^{2-}] = [G^{-1}] 232 = \boxed{9.76 \times 10^{16} \text{ cm}^{-3}}$$

$$[G_0] = \frac{[G^-]}{2.6 \times 10^{18}} = \boxed{1.62 \times 10^{-4} \text{ cm}^{-3}}$$

e. From c and d, $4.21 \times 10^{14} \text{ cm}^{-3}$ G atoms have accepted 1 e^- , and $9.76 \times 10^{16} \text{ cm}^{-3}$ have accepted 2 e^- , so: $E_f = E_i + kT \ln (N_d + 2[G^{2-}] + [G^{-1}]) = \boxed{1.14 \text{ eV}}$
or an error of 0.1 eV, which is not so bad. n_i

6. First we need $[V_0]$: $[V_0] = N e^{\Delta S_{vib}/k_B} e^{-\Delta E_{vac}/kT}$

Assuming $\Delta S_{vib} = 1.1 k_B$, $[V_0^B] = 9.48 \times 10^{11} \text{ cm}^{-3}$, $[V_0^C] = 2.38 \times 10^6 \text{ cm}^{-3}$

$$[V^{B+}] = [V_0^B] e^{-(E_f - E_{B^+})/kT}, \quad E_{B^+} = 1.3 \text{ eV} - 0.45 \text{ eV}, \text{ so } [V^{B+}] = 5.45 \times 10^9 \text{ cm}^{-3}$$

$$[V^{C-}] = [V_0^C] e^{(E_f - E_{C-})/kT} = 7.19 \times 10^{10} \text{ cm}^{-3}$$

so $[V^B] = [V^{B+}] + [V_0^B] = \boxed{9.53 \times 10^{11} \text{ cm}^{-3}}$, $[V^C] = [V^{C-}] + [V_0^C] = \boxed{7.19 \times 10^{10} \text{ cm}^{-3}}$

20/20

4.5)

7. The misfit $f = \frac{|a_s - a_f|}{a_s}$. For GaAs: $f = 0.0124$
 For InP: $f = 0.0256$

8. For a 60° type misfit dislocation $\theta = \phi = 60^\circ$, and the critical thickness can be found by solving

$$h/b = \frac{1 - \nu \cos^2 \theta}{8\pi f (1 + \nu) \cos \theta} \ln\left(\frac{dh_c}{b}\right)$$
 With $\alpha = 1$, $\nu = 0.29$, this is solved numerically as

$$\frac{h_c}{b} = 11.11$$

a. Dislocations would be introduced into the film by some form of dislocation multiplication if the thickness is much greater than the critical thickness. Generally the dislocation multiplication is enabled by threading dislocations. One example of this is the Frank-Read mechanism. In this case a misfit dislocation is pinned by 2 threading segments, and as it grows the misfit dislocation separates out and creates a new dislocation. This happens when there is large stress, which is the case for $t \gg t_c$.

10. a. Between these 3, a perfect edge dislocation provides the maximum strain relief for the same dislocation line energy. This can be seen because, equivalently, for the same strain relief $E_{dis} \propto 1 - \nu \cos^2 \theta$, so for an edge $\theta = 0^\circ$ and E_{dis} is the smallest possible. This means if the dislocation energy is the same, an edge dislocation provides more strain relief.

b. A 60° misfit dislocation is most likely to form because edge dislocations are the most energetically favorable, growth while occurs on $\{001\}$ planes which are most favorable, while growth occurs on $\{111\}$ planes which are less favorable. So the smallest angle dislocations can form on $\{111\}$ planes.

11. The depletion radius from a single threading dislocation is

$$R = \sqrt{\frac{f \sin \alpha}{N_d a \pi}}$$

For edge dislocations $\alpha = \pi/2$, $a =$

$f = 1$, $a = 0.357 \text{ nm}$ in this case, so

$$R = 7.1 \times 10^{-5} \text{ cm}$$

✓
 $\sqrt{2}/2$

Sanjeev Kolli

ECE5570HW4

#1

PROB1

- a) Goldstone modes are slow long range fluctuations in a given order parameter. They originate from a no barrier transition, i.e. there is no energy cost for the fluctuations. A symmetric phase at high temperature separates into two asymmetric phases. An example in Semiconductors is the existence of spin waves

b) $S(q) = \frac{1}{N} \left| \sum_j e^{iq \cdot \vec{R}_j} \right|^2$ $\vec{R}_j = ja$ Geometric Series

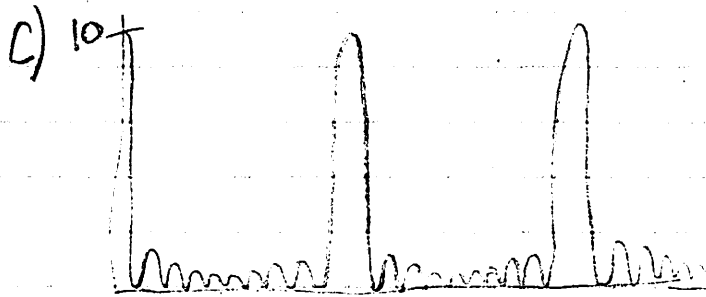
$$\begin{aligned} &= \frac{1}{N} \left| \frac{1 - e^{iqaN}}{1 - e^{iqa}} \right|^2 \\ &= \frac{1}{N} \frac{(1 - e^{iqaN})(1 - e^{-iqaN})}{(1 - e^{iqa})(1 - e^{-iqa})} \\ &= \frac{1}{N} \frac{(2 - e^{iqaN} - e^{-iqaN})}{(2 - e^{iqa} - e^{-iqa})} \\ &= \frac{1}{N} \frac{2(1 - \cos(qaN))}{2(1 - \cos qa)} \\ &= \frac{1}{N} \frac{\sin^2\left(\frac{qaN}{2}\right)}{\sin^2\left(\frac{qa}{2}\right)} \end{aligned}$$

Sanjeev Kolli

ECE5570HW4

#2

PROB 1 cont.



Satellite peaks = 8 (N-2)



Max height = 100

$$\sin^2\left(\frac{qaN}{2}\right) = 0$$

$$qa\frac{N}{2} = \pi$$

$qa = \frac{2\pi}{N}$ indicates
N ways to get
zeros

N satellite peaks

$$S(q) = \frac{1}{N} \left(\frac{\sin \frac{qaN}{2}}{\sin \frac{qa}{2}} \right)^2$$

$$S'(qa) = \frac{2}{N} \left(\frac{\sin \frac{qaN}{2}}{\sin \frac{qa}{2}} \right) \frac{N \sin \frac{qa}{2} \cos \frac{qaN}{2} - \frac{1}{2} \sin \frac{qaN}{2} \sin \frac{qa}{2}}{\sin^2 \frac{qa}{2}}$$

$$\lim_{qa \rightarrow 0} \frac{1}{N} \left(\frac{\sin \frac{qaN}{2}}{\sin \frac{qa}{2}} \right)^2 = \frac{1}{N} \left(\frac{N}{1} \right)^2 = \frac{1}{N}$$

to

Sanjeev Kulli ELES570HW4

#3

PROB 1 cont.

- d) Maximum peak strength is ~ 5 , still 10 peaks in between
 Peak height and width for $N=100$ is roughly the same
 No, when defects are low in concentration they have only minor effects on diffraction experiments.

PROB 2

$$\begin{aligned}
 f(q) &= \frac{1}{N} \sum_j e^{i q \cdot \vec{r}_j + \vec{u}_j(t)} \\
 &= \frac{1}{N} \sum_j e^{i q \cdot \vec{r}_j} \langle e^{i q \cdot \vec{u}_j(t)} \rangle \\
 &= \frac{1}{N} \sum_j e^{i q \cdot \vec{r}_j} e^{\frac{1}{2} \langle (i \vec{q} \cdot \vec{u}_j)^2 \rangle} \\
 &= \frac{1}{N} \sum_j e^{i q \cdot \vec{r}_j} e^{-\frac{1}{2} \langle (\vec{q} \cdot \vec{u}_j)^2 \rangle} \\
 S(q) &= \frac{1}{N} \left| \sum_j e^{i q \cdot \vec{r}_j} e^{-\frac{1}{2} \langle (\vec{q} \cdot \vec{u}_j)^2 \rangle} \right|^2 \\
 &= \frac{1}{N} \left(\sum_j e^{i q \cdot \vec{r}_j} e^{-\frac{1}{2} \langle (\vec{q} \cdot \vec{u}_j)^2 \rangle} \right) \cdot \left(\sum_k e^{-i q \cdot \vec{r}_k} e^{\frac{1}{2} \langle (\vec{q} \cdot \vec{u}_k)^2 \rangle} \right) \\
 &= \frac{1}{N} \sum_{j,k} e^{i q \cdot (\vec{r}_j - \vec{r}_k)} \cdot \prod_{j,k} e^{\frac{1}{2} \langle (\vec{q} \cdot \vec{u}_j)^2 \rangle} e^{-\frac{1}{2} \langle (\vec{q} \cdot \vec{u}_k)^2 \rangle} \\
 &= S(q, T=0) \cdot \prod_{j,k} \langle e^{i \vec{q} \cdot \vec{u}_j} \rangle \cdot \langle e^{-i \vec{q} \cdot \vec{u}_k} \rangle \\
 &= S(q, T=0) \cdot \sum_k e^{i q \cdot (\vec{u}_j - \vec{u}_k)}
 \end{aligned}$$

Sanjeev Kollu

ELSS570 HW4

#4

PROB 2 cont.

$$\begin{aligned}
 b) \left\langle e^{iq \sum_{jk} (u_j(t) - u_k(t))} \right\rangle &= e^{\frac{1}{2} \left\langle \left(iq \sum_{jk} (u_j(t) - u_k(t)) \right)^2 \right\rangle} = \\
 &= e^{-\frac{1}{2} q^2 \langle dx^2 \rangle} \rightarrow \begin{aligned} &U = \frac{1}{2} k dx^2 \rightarrow \langle U \rangle = \frac{1}{2} k \langle dx^2 \rangle \\ &\langle U \rangle = k_B T \rightarrow \langle dx^2 \rangle = \frac{k_B T}{\frac{1}{2} k} = \frac{k_B T}{\frac{1}{2} \omega_0^2 M} \end{aligned} \\
 &= e^{-\frac{1}{2} \left(\frac{2 k_B T}{\omega_0^2 M} \right) q^2} \\
 &= e^{\left(\frac{-k_B T q^2}{\omega_0^2 M} \right)} \checkmark
 \end{aligned}$$

$\sqrt{\frac{k}{M}} = \omega_0 \quad k = \omega_0^2 M$

$$c) S(q) = \frac{1}{N} \frac{\sin^2 Naq}{\sin^2 aq} e^{\left(\frac{-k_B T q^2}{M \omega_0^2} \right)}$$

The Debye Waller factor decreases the intensity of higher order peaks. Yes this makes intuitive sense higher order peaks are more affected by fluctuations

d) on plots section

e) Yes one could use this temperature dependence as a thermometer for a crystal. Semiconductors with large masses and high vibrational frequencies would allow for a slow decay for easy observation.

Sanjeer Koll

ECESS/OTW4

#5

PROB 3

a) $\alpha_0 = 1 \quad \alpha_1 = 4 \quad \alpha_2 = 6 \quad \alpha_3 = 4 \quad \alpha_4 = 1$

$q_0 = (1-x)^4 \quad q_1 = x(1-x)^3 \quad q_2 = x^2(1-x)^2 \quad q_3 = x^3(1-x) \quad q_4 = x^4$

For Random case these quantities by just statistical entropic number of states.

For calculating strain energy of tetrahedra

$U_{\triangle} = U_{\text{str}} + U_{\text{bnd}}$ combination of bend/stretch Strain

$U_{\text{str}} = \sum_{i=1}^4 U_{\text{str},i}$ 4 bonds to consider per tetrahedra

$U_{\text{bnd}} = 2 \sum_{i=1}^4 \sum_{j>i}^4 U_{\text{bnd},ij}$ 6 bending angles to consider

$U_{\text{str},i} = \frac{3}{8} \alpha_i \frac{(d_i^2 - d_{i,0}^2)^2}{d_{i,0}^2} \quad U_{\text{bnd},ij} = \frac{3}{8} \frac{\beta_i + \beta_j}{2} \frac{(\vec{d}_i \cdot \vec{d}_j - d_{i,0} d_{j,0})^2}{d_{i,0} d_{j,0}}$

U_{\triangle} was calculated for each tetrahedra type as a function of global composition x .

Then minimizing Free energy resulted in finding equilibrium q values with Lagrange multipliers.

$q_i^0 = C \eta_i t^{4-i} \quad \eta_i$ represents Boltzmann distribution as a function of strain energy

$(1-x)\eta_0 t^4 + (3-4x)\eta_1 t^3 + (3-6x)\eta_2 t^2 + \dots + (1-4x)\eta_3 t + x\eta_4 = 0$
 $e^{-E_i/KT}$
 C is normalization constant so $\sum \eta_i = 1$
 t represents inter type relationships

Sanjeev Kollu

ECES578

#6

PROB 3 cont.

β represents order parameter and is calculated
$$\beta = 1 - \frac{q_1 + 2q_2 + q_3}{x(1-x)}$$
 after considering A-B pairs in a given tetrahedron
negative β represents favoring of A-B being together rather than A-A or B-B.

With all these quantities Figures 3-5 could be recreated (Results shown on attached graphs)

b) The deposition of III-V ternary alloys shows that ordering is preferred over clustering. This is because tetrahedra in the Zinc-Blende structure further from the average composition have higher strain energy. The reduction in strain energy due to long range ordering of the average composition tetrahedra is not as much of an effect at higher temperatures due to the preference of a high entropy system.

c)

AlGaAs	pHEMT based MMIC for communications
InGaAs	pHEMT based MMIC for communications
InGaP	Top layer for 4+ multilayer solar cells
AlGaSb	Infrared Optical Devices
InGaSb	high mobility channels for CMOS enhancement
GaAsP	Red LEDs / Solar Cells
GaAsSb	DHBT > 700 GHz power gain cutoff
GaPSb	HBT / High Power Devices
InAsP	Photodetectors at long wavelengths
InPSb	Mid Infrared Photodetectors
InAsSb	High mobility transistor channels

Sanjeev Kollu

ECE5570 HW4

#7

PROB4

1) i) Charge balance $n + G^- = p$
 $N_A e^{-(E_F - E_V)/KT} + N_G e^{(E_G - E_F)/KT} = N_A e^{-(E_F - E_V)/KT}$
 $E_F = 0.075$

ii) G^+ charge is mostly -
 V_B^+ is mostly +1 because the occupation state is above the Fermi level and unoccupied corresponds to +1 charge. V_C^- is mostly neutral because V_C^- is above Fermi level and unoccupied corresponds to neutral charge.

2) V_B^+ is more common because the negatively charged G atoms seek charge balance with the vacancies. Instead of taking from the valence band.

3) Traps because recombination centers would require an electron hole pair the G atoms would be likely doubly negatively charged acting as an electron sink preventing recombination.

4) a) B sites

b) Lesser tendency due to lower ionization energy

c) G due to its multiple charge states within the gap

Sanjeev Kollu

ECE5570 HW 4

8

PROB 4 cont

$$5) a) E_F = 0.65 \text{ eV} + (8.617 \times 10^{-5}) (300 \text{ K}) (\ln(1 \times 10^{10}))$$

$$= \boxed{1.245 \text{ eV}} \text{ above valence band edge}$$

$$b) \frac{[G^-]}{[G_0]} = e^{(1.245 - 0.15) / (8.617 \times 10^{-5}) (300 \text{ K})}$$

$$= \boxed{2.5 \times 10^{18}}$$

$$c) \frac{[G^{2-}]}{[G^-]} = e^{(1.245 - 1.10) / (8.617 \times 10^{-5}) (300 \text{ K})}$$

$$= \boxed{273}$$

$$d) [G_0] + 2.5 \times 10^{18} [G_0] + 273 (2.5 \times 10^{18}) [G_0] = 9.8 \times 10^{16}$$

$$274 (2.5 \times 10^{18}) [G_0] = 9.8 \times 10^{16} \quad \left([G_0] = 1.4 \times 10^{-4} \text{ cm}^{-3} \right)$$

$$\boxed{\begin{aligned} [G^-] &= 3.58 \times 10^{14} \text{ cm}^{-3} \\ [G^{2-}] &= 9.76 \times 10^{16} \text{ cm}^{-3} \end{aligned}}$$

$$e) E_F = 0.65 \text{ eV} + (8.617 \times 10^{-5}) (300 \text{ K}) (\ln((2 \times 10^{17} - (1.956 \times 10^{17})) / 2 \times 10^{17}))$$

$$= 0.65 + .514$$

$$= 1.164 \text{ eV above valence band edge}$$

$$\boxed{\Delta E_{\text{error}} = .081 \text{ eV}}$$

Sanjeev Kollu ECE5570 HW4

#9

PROB 4 cont

$$6) [V_a^0] = N e^{(\Delta S_{vib}/k_B)} e^{-\Delta E_{vac}/k_B T}$$

$$\frac{[V_a^-]}{[V_a^0]} = e^{(E_F - E_{V_a^-})/k_B T}$$

$$[V_B^0] = N e^{(\Delta S_{vib}/k_B)} e^{-\Delta E_{vac,B}/k_B T}$$

$$\frac{[V_B^+]}{[V_B^0]} = e^{(E_{V_B^+} - E_F)/k_B T}$$

PROBS

$$7) f_{F, \text{GaAs}} = \frac{.572 - .565}{.565} = .0124$$

$$f_{\text{InP}} = \frac{.572 - .587}{.587} = -.0256$$

8)

$$E_{el} = f E_{dis}$$

$$\frac{2G(1+\nu)}{(1-\nu)} f^2 h = f \frac{Gb^2}{4\pi} \frac{1-\nu \cos^2(\theta)}{1-\nu} \ln\left(\frac{ah}{b}\right)$$

$$\frac{hc/b}{\ln(ah/b)} = \frac{1-\nu \cos^2 \theta}{8\pi f(1+\nu) \cos \phi} = \frac{1-(.29)(\cos 68^\circ)^2}{8\pi (.0124)(1+.29) \cos(60^\circ)} = 4.614$$

$$\frac{h_e}{b} = 11.109 \quad (1.235)$$

PROB 5 cont.

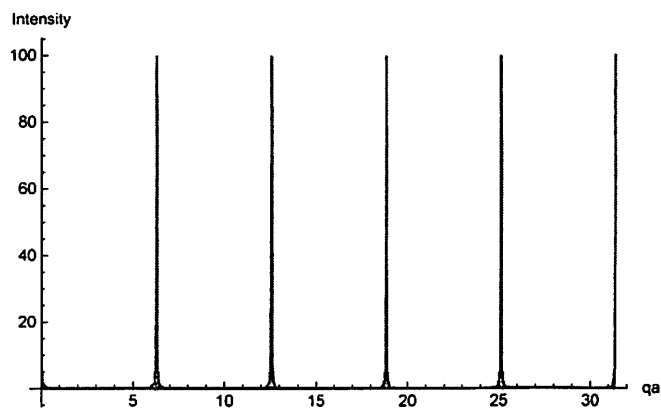
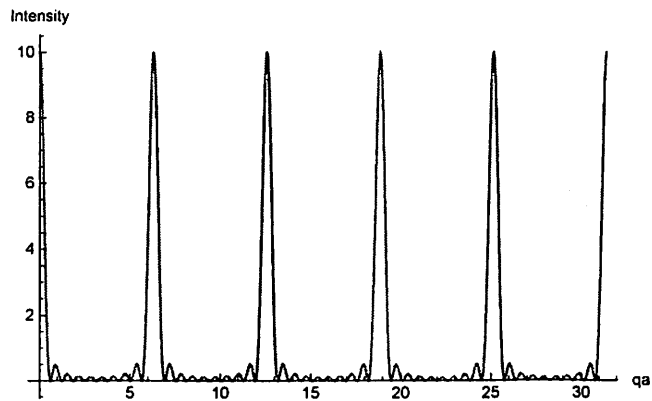
9) Threading dislocation segments are the most common way of introducing dislocations past the critical thickness. This happens by extension of existing dislocations to newly forming surfaces.

10) a) The perfect edge dislocation

b) The 60° partial dislocation because it is actually possible to form (Burger's is in glide plane) and it releases more energy than the screw dislocation.

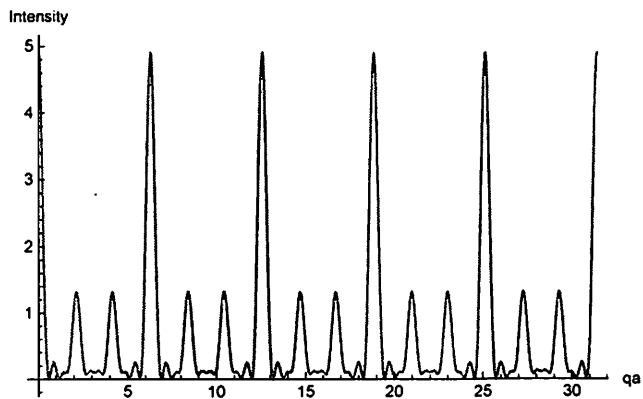
$$11) R = \sqrt{\frac{f}{a\pi N_d}} = \sqrt{\frac{1}{(0.572)(\pi)(1.1 \times 10^{15} \text{ cm}^{-3})}} = 711.3 \text{ nm}$$

1c)

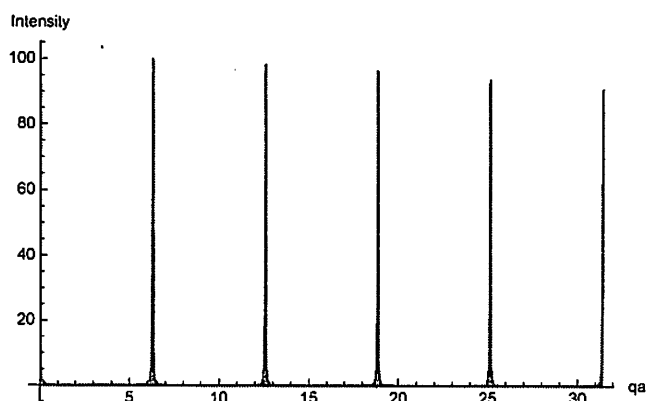
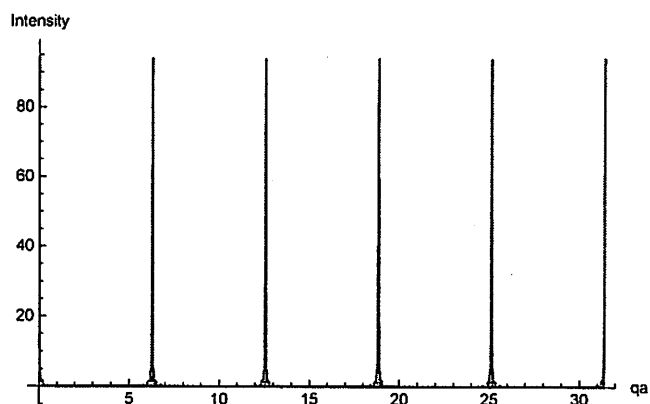


vacatestruct[n_, j_, k_, l_] :=
 1 / n * (Abs[(Sum[E^(I * x * a), {a, 1, j}] + Sum[E^(I * x * a), {a, j + 2, k}] +
 Sum[E^(I * x * a), {a, k + 2, l}] + Sum[E^(I * x * a), {a, l + 2, n}]))^2;

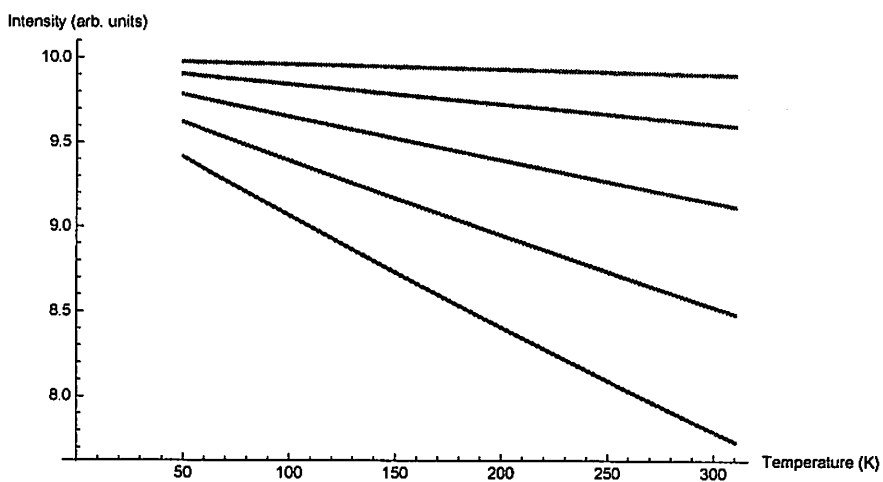
1d)



1d)



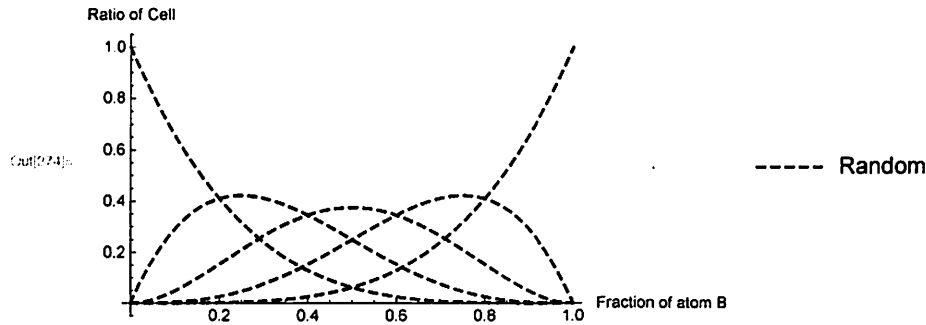
2d)



```

In[274]:= randomqs = Plot[{(1 - x)^4, 4 * x * (1 - x)^3, 6 * x^2 * (1 - x)^2, 4 * x^3 * (1 - x), x^4},
  {x, 0, 1}, PlotRange -> All, PlotLegends -> {"Random"}, AxesLabel ->
  {"Fraction of atom B", "Ratio of Cell"}, PlotStyle -> {{Black, Dashed}}]

```



```

In[13]:= Solve[4.614 * Log[x] - x == 0, x]

```

```

Out[13]:= {{x -> 1.33576}, {x -> 11.1097}}

```

```

αGaAs = 41.19;

```

```

βGaAs = 8.95;

```

```

αInAs = 35.18;

```

```

βInAs = 5.50; aGaAs = 5.6533 * 10^-10;

```

```

aInAs = 6.0584 * 10^-10; dGaAs0 = √3 / 4 * aGaAs; dInAs0 = √3 / 4 * aInAs;

```

```

aVC[x_] := ((x) * aGaAs + (1 - x) * aInAs);

```

```

thetaT = 2 * ArcTan[√2];

```

```

In[453]:= dGaAs3[x_] := ((aVC[x] / 4 - z3)^2 + aVC[x]^2 / 8)^0.5;

```

```

dInAs3[x_] := ((aVC[x] / 4 + z3)^2 + aVC[x]^2 / 8)^0.5;

```

```

cosGaAsGa3[x_] := (aVC[x]^2 / 2 - 2 * dGaAs3[x]^2) / (2 * dGaAs3[x]^2);

```

```

cosInAsIn3[x_] := (aVC[x]^2 / 2 - 2 * dInAs3[x]^2) / (2 * dInAs3[x]^2);

```

```

alttetstrain5050[x_] := 3 / 4 * αGaAs * (dGaAs3[x]^2 - dGaAs0^2)^2 / dGaAs0^2 +
  3 / 4 * αInAs * (dInAs3[x]^2 - dInAs0^2)^2 / dInAs0^2 + 3 / 4 * βGaAs *
  (dGaAs3[x]^2 * cosGaAsGa3[x]^2 - dGaAs0^2 * Cos[thetaT]^2)^2 / dGaAs0^2 + 3 / 4 *
  βInAs * (dInAs3[x]^2 * cosInAsIn3[x]^2 - dInAs0^2 * Cos[thetaT]^2)^2 / dInAs0^2;

```

```

In[453]:= tetstrain5050solver[x_] :=
  alttetstrain5050[x] /. FindRoot[D[alttetstrain5050[x], z3], {z3, 0}][[1]]

```

```

In[129]:= tetstrain1000[x_] := 3 / 2 * αGaAs * (3 / 16 * aVC[x]^2 - dGaAs0^2)^2 / dGaAs0^2;

```

```

In[130]:= tetstrain0100[x_] := 3 / 2 * αInAs * (3 / 16 * aVC[x]^2 - dInAs0^2)^2 / dInAs0^2;

```

```

in[220]:= ustr2575[x_] := 9/8 *  $\alpha$ InAs * (dInAs[x]^2 - dInAs0^2)^2/dInAs0^2 +
          3/8 *  $\alpha$ GaAs * (dGaAs[x]^2 - dGaAs0^2)^2/dGaAs0^2;

dInAs[x_] :=  $\sqrt{\left(aVC[x]/2 * \sqrt{2/3}\right)^2 + \left(aVC[x]/4/\sqrt{3} + z1\right)^2}$ ;
dGaAs[x_] :=  $\sqrt{3}/4 * aVC[x] - z1$ ;
thetaT = 2 * ArcTan[ $\sqrt{2}$ ];
tetredge[x_] := aVC[x]/ $\sqrt{2}$ ;
ubnd2575[x_] := 9/4 * ( $\beta$ GaAs +  $\beta$ InAs) / 2 *
  (dInAs[x] * dGaAs[x] * cosGaAsIn[x]^2 - dInAs0 * dGaAs0 * Cos[thetaT]^2)^2/dInAs0 /
  dGaAs0 + 9/4 *  $\beta$ InAs *
  (dInAs[x]^2 * cosInAsIn[x]^2 - dInAs0^2 * Cos[thetaT]^2)^2/dInAs0^2;
tetstrain2575[x_] := ustr2575[x] + ubnd2575[x];
cosGaAsIn[x_] :=
  (tetredge[x]^2 - dGaAs[x]^2 - dInAs[x]^2) / (2 * dGaAs[x] * dInAs[x]);
cosInAsIn[x_] := (tetredge[x]^2 - 2 * dInAs[x]^2) / (2 * dInAs[x]^2);
tetstrain2575solver[x_] :=
  tetstrain2575[x] /. FindRoot[D[tetstrain2575[x], z1], {z1, 0}][[1]];

ustr7525[x_] := 3/8 *  $\alpha$ InAs * (dInAs2[x]^2 - dInAs0^2)^2/dInAs0^2 +
          9/8 *  $\alpha$ GaAs * (dGaAs2[x]^2 - dGaAs0^2)^2/dGaAs0^2;

dGaAs2[x_] :=  $\sqrt{\left(aVC[x]/2 * \sqrt{2/3}\right)^2 + \left(aVC[x]/4/\sqrt{3} + z2\right)^2}$ ;
dInAs2[x_] :=  $\sqrt{3}/4 * aVC[x] - z2$ ;
tetredge[x_] := aVC[x]/ $\sqrt{2}$ ;
ubnd7525[x_] := 9/4 * ( $\beta$ GaAs +  $\beta$ InAs) / 2 *
  (dInAs2[x] * dGaAs2[x] * cosGaAsIn2[x]^2 - dInAs0 * dGaAs0 * Cos[thetaT]^2)^2 /
  dInAs0 / dGaAs0 + 9/4 *  $\beta$ GaAs *
  (dGaAs2[x]^2 * cosGaAsGa2[x]^2 - dGaAs0^2 * Cos[thetaT]^2)^2/dGaAs0^2;
tetstrain7525[x_] := ustr7525[x] + ubnd7525[x];
cosGaAsIn2[x_] :=
  (tetredge[x]^2 - dGaAs2[x]^2 - dInAs2[x]^2) / (2 * dGaAs2[x] * dInAs2[x]);
cosGaAsGa2[x_] := (tetredge[x]^2 - 2 * dGaAs2[x]^2) / (2 * dGaAs2[x]^2);
tetstrain7525solver[x_] :=
  tetstrain7525[x] /. FindRoot[D[tetstrain7525[x], z2], {z2, 0}][[1]];

```

```

In[161]:= p1 = Plot[6.02*^23/4186*tetstrain0100[x], {x, 0, 1}, PlotRange -> {{0, 1}, {0, 15}},
  AxesLabel -> {"Composition x", "Strain Energy (kcal/mol)"}];
p2 = Plot[6.02*^23/4186*tetstrain2575solver[x],
  {x, 0, 1}, PlotRange -> {{0, 1}, {0, 15}}];
p3 = Plot[6.02*^23/4186*tetstrain5050solver[x],
  {x, 0, 1}, PlotRange -> {{0, 1}, {0, 15}}];
p5 = Plot[6.02*^23/4186*tetstrain1000[x], {x, 0, 1}, PlotRange -> {{0, 1}, {0, 15}}];
p4 = Plot[6.02*^23/4186*tetstrain7525solver[x],
  {x, 0, 1}, PlotRange -> {{0, 1}, {0, 15}}];
Show[{p1, p2, p3, p4, p5}]

```

Strain Energy (kcal/mol)

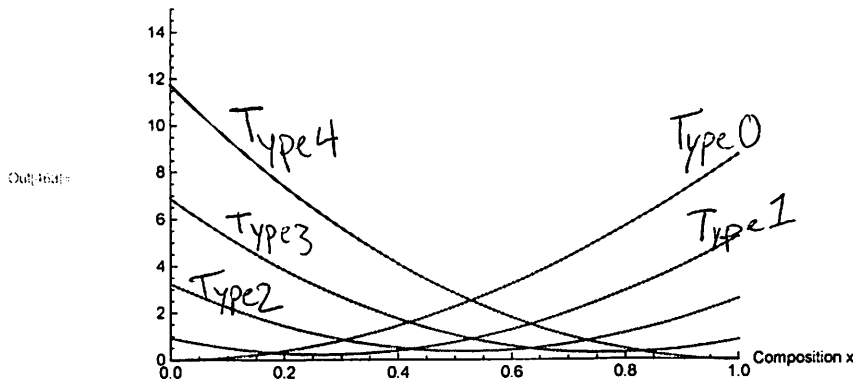


Fig 2 from
paper

```

In[164]:= tsolver[x_, temp_] :=
  t /. Solve[{(1 - x) * E^(-tetstrain1000[x] / (1.38*^-23) / temp) * t^4 +
    (3 - 4 * x) * E^(-tetstrain7525solver[x] / (1.38*^-23) / temp) * t^3 +
    (3 - 6 * x) * E^(-tetstrain5050solver[x] / (1.38*^-23) / temp) * t^2 +
    (1 - 4 * x) * E^(-tetstrain2575solver[x] / (1.38*^-23) / temp) * t -
    x * E^(-tetstrain0100[x] / (1.38*^-23) / temp) == 0, t > 0}, t][[1]];

In[165]:= constant[x_, temp_] :=
  (E^(-tetstrain1000[x] / (1.38*^-23) / temp) * tsolver[x, temp]^4 +
    E^(-tetstrain7525solver[x] / (1.38*^-23) / temp) * tsolver[x, temp]^3 * 4 +
    E^(-tetstrain5050solver[x] / (1.38*^-23) / temp) * tsolver[x, temp]^2 * 6 +
    E^(-tetstrain2575solver[x] / (1.38*^-23) / temp) * tsolver[x, temp] * 4 +
    E^(-tetstrain0100[x] / (1.38*^-23) / temp))^(-1);

In[166]:= q0[x_, temp_] :=
  constant[x, temp] * E^(-tetstrain1000[x] / (1.38*^-23) / temp) * tsolver[x, temp]^4;
q1[x_, temp_] := constant[x, temp] *
  E^(-tetstrain7525solver[x] / (1.38*^-23) / temp) * tsolver[x, temp]^3;
q2[x_, temp_] := constant[x, temp] * E^(-tetstrain5050solver[x] / (1.38*^-23) / temp) *
  tsolver[x, temp]^2;
q3[x_, temp_] := constant[x, temp] * E^(-tetstrain2575solver[x] / (1.38*^-23) / temp) *
  tsolver[x, temp];
q4[x_, temp_] := constant[x, temp] * E^(-tetstrain0100[x] / (1.38*^-23) / temp);

```



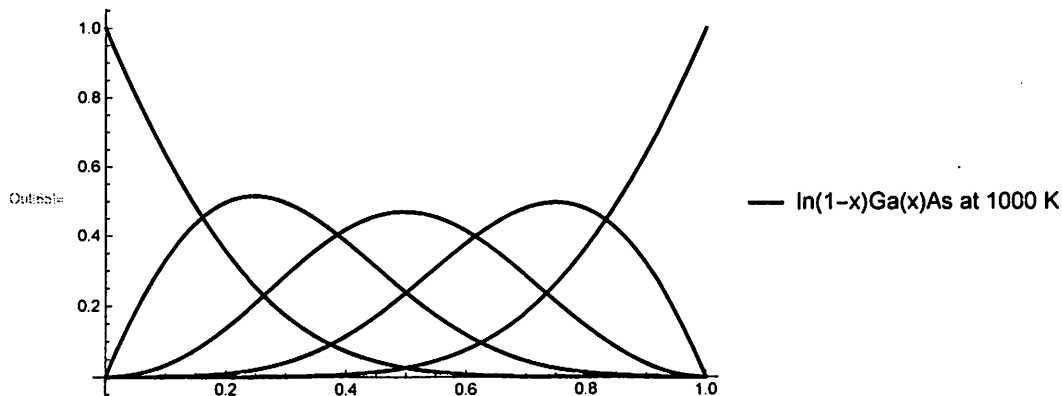
```

In[49]:= constant[x_, temp_] :=
  (E^(-tetstrain1000[x] / (1.38*^-23) / temp) * tsolver[x, temp]^4 +
   E^(-tetstrain7525solver[x] / (1.38*^-23) / temp) * tsolver[x, temp]^3 +
   E^(-tetstrain5050solver[x] / (1.38*^-23) / temp) * tsolver[x, temp]^2 +
   E^(-tetstrain2575solver[x] / (1.38*^-23) / temp) * tsolver[x, temp] +
   E^(-tetstrain0100[x] / (1.38*^-23) / temp))^(-1);

In[50]:= q0[x_, temp_] :=
  constant[x, temp] * E^(-tetstrain1000[x] / (1.38*^-23) / temp) * tsolver[x, temp]^4;
q1[x_, temp_] := constant[x, temp] *
  E^(-tetstrain7525solver[x] / (1.38*^-23) / temp) * tsolver[x, temp]^3;
q2[x_, temp_] := constant[x, temp] * E^(-tetstrain5050solver[x] / (1.38*^-23) / temp) *
  tsolver[x, temp]^2;
q3[x_, temp_] := constant[x, temp] * E^(-tetstrain2575solver[x] / (1.38*^-23) / temp) *
  tsolver[x, temp];
q4[x_, temp_] := constant[x, temp] * E^(-tetstrain0100[x] / (1.38*^-23) / temp);

In[55]:= weightedqs = Plot[
  {q0[x, 1000], 4 * q1[x, 1000], 6 * q2[x, 1000], 4 * q3[x, 1000], q4[x, 1000]}, {x, 0, 1},
  PlotStyle -> {{Black, Thick}}, PlotLegends -> {"In(1-x)Ga(x)As at 1000 K"}]

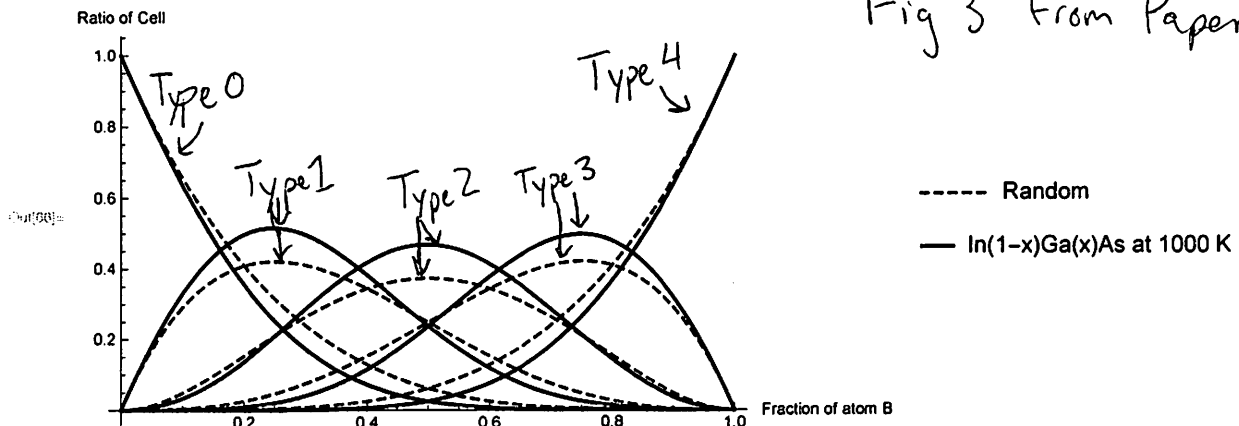
```



```

In[60]:= Show[{randomqs, weightedqs}]

```



The above graph shows the difference in distribution of tetrahedra types between random arrangement of Type 0-4 tetrahedra and an actual material, $\text{In}_{1-x}\text{Ga}_x\text{As}$ at 1000K. The real material shows more preference for a given tetrahedra that matches its global composition compared to the random arrangement. This is due to the differences in energies of the tetrahedra due to strain.

```
In[57]:= orderParam[x_, temp_] := 1 - (q1[x, temp] + 2 * q2[x, temp] + q3[x, temp]) / x / (1 - x);
```

```
fig4 = Plot[{orderParam[x, 500], orderParam[x, 1000], orderParam[x, 2000]},  
{x, 0, 1}, AxesLabel -> {"Composition x", "Order Parameter  $\beta$ "},  
PlotLegends -> {"500 K", "1000 K", "2000 K"}, PlotRange -> {{0, 1}, {-0.4, 0}}]
```

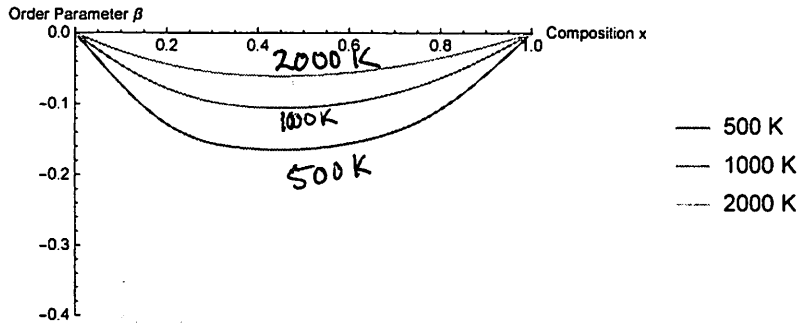
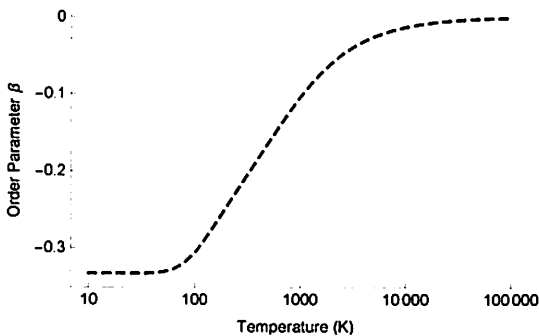


Fig 4 from paper

The above plot shows the difference in order parameter given temperature and composition. A more negative order parameter represents more order in the structure. At lower temperatures, there is a preference for more long range ordering of tetrahedra because at lower temperature enthalpy is more important to lower the free energy. At higher temperatures increasing configurational entropy is more important lower free energy so ordering is not as preferred. As the composition of the InGaAs mixture approaches 50:50 the tetrahedra have more configurational coordination in order to lower the energy.

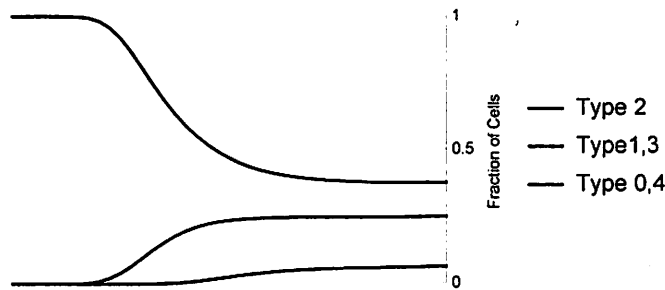
```
olist = Table[{10^(i/10), orderParam[0.5, 10^(i/10)]}, {i, 10, 50}];
```



```
q2list = Table[{10^(i/10), 6 * q2[0.5, 10^(i/10)]}, {i, 10, 50}];
```

```
q1list = Table[{10^(i/10), 4 * q1[0.5, 10^(i/10)]}, {i, 10, 50}];
```

```
q0list = Table[{10^(i/10), q0[0.5, 10^(i/10)]}, {i, 10, 50}];
```



```
fig5 = Overlay[{oplot, qsplot}, Alignment -> {Top, Top}]
```

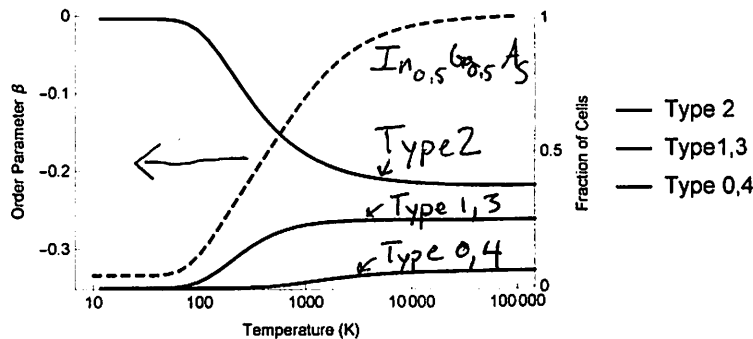


Fig 5 from paper

The above plot shows the effect of temperature on order parameter and type of tetrahedra present in an $\text{In}_{0.5}\text{Ga}_{0.5}\text{As}$ compound. As seen in the previous figure, increasing temperature results in order parameter approaching 0 due to the favoring of configurational entropy/randomness at high temperatures. At low temperatures the Type 2 tetrahedra (50:50 split) are highly favored because they have the lowest strain energy given the global composition. As temperature is increased, more randomness in the tetrahedra composition can occur and other types of tetrahedra can exist. At very high temperatures, the compound approaches the random approximation seen in the duplication of Figure 3. All tetrahedras begin to occur based solely on configurational statistics rather than considering the strain energy of the each tetrahedra.